Iron overload reduces adiponectin receptor-1 expression
via a ROS/FOXO1-dependent mechanism leading to
adiponectin resistance in skeletal muscle cells

Karam Dahyaleh

A Thesis submitted to the Faculty of Graduate Studies in
Partial Fulfillment of the Requirements for the Degree of
Master of Science

Graduate Program in Biology
York University
Toronto, Ontario
August 2019

Abstract

Iron overload (IO) is a common yet underappreciated observation in metabolic syndrome (MetS) patients. With the prevalence of MetS continuing to rise, it is of utmost importance to further elucidate mechanisms leading to metabolic dysfunction. IO positively correlates with reduced circulating adiponectin levels yet the impact of IO on adiponectin action is unknown. Here, we established a model of IO in L6 skeletal muscle cells and found that it induced adiponectin resistance, measured by reduced P38 MAPK phosphorylation by the adiponectin receptor (AdipoR) agonist AdipoRon. This correlated with reduced mRNA and protein levels of AdipoR1 and its facilitative binding partner APPL1. IO caused phosphorylation, nuclear extrusion and inhibition of FOXO1, a known transcription factor for AdipoR1. Reactive oxygen species production was induced by IO and using N-acetyl cysteine (NAC) to prevent this attenuated the effect of IO in FOXO1 phosphorylation, localization and adiponectin resistance. In conclusion, our study identifies a ROS/FOXO1/AdipoR1 axis as a cause of skeletal muscle adiponectin resistance in response to IO. This new knowledge provides new insight on potential disease pathophysiology in MetS patients with IO.

Acknowledgements

Table of Contents

List of figures

List of Abbreviations

ACC Acetyl-CoA (Coenzyme A) carboxylate

AdipoR1 Adiponectin receptor 1

AdipoR2 Adiponectin receptor 2

AdipRon AdipoRon

Akt Protein kinase B

AMP Adenosine monophosphate

AMPK Adenosine monophosphate-activated protein kinase

APPL1 Leucine zipper motif

ATP Adenosine TriPhosphate

BMI Body Mass Index

BSA Bovine serum albumin

CaMKK Ca^{2+}/calmodulin-dependent protein kinase kinase

CBP/p300 CREB Binding Protein

CDK1/2 Cyclin-dependent kinase 1

CoA Coenzyme A

CRP C reactive protein

DCTB Duodenal cytochrome B

DIOS Dysmetabolic iron overload syndrome

DMSO Dymethyl sulfoxide

DMT1 Divalent metal-ion transporter 1

DsbA-L disulfide bond A oxidoreductase-like

ER Endoplasmic reticulum

Ero-1La ER oxidoreductase -1La

ETC Electron transport chain

fAd Full length adiponectin

FBS Fetal bovine serum

FOXO1 Forkhead box protein O1

gAd Globular adiponectin

GLUT4 Glucose transporter type 4

GPCR G protein coupled receptor

GTT Glucose tolerance test

HDL High density lipids

HJV Hemojuvelin

HMW High molecular weight

HRP Secondary horseradish peroxidase

IDF International diabetes federation

IL-6 Interleukin 6

IR Insulin receptor

IRS1/2 Insulin receptor substrate 1/2

IO Iron overload

IRE-CFP Iron response element - cyan fluorescent protein

IRP Iron response protein

JNK c-Jun N-terminal kinases

kDa Kilodalton

KO Knockout

LMW Low molecular weight

LDL Low density lipids

LPL Lipoprotein lipase

MAPK mitogen-activated protein kinases

MMW Middle molecular weight

MST 1 mammalian Ste20-like kinase 1

NADPH Nicotinamide adenine dinucleotide phosphate

NHNES National Health and Nutrition Education Survey

NCEP:ATP III National Cholesterol Education Program's Adult Treatment Panel III

NEFA Non esterified fatty acids

NES Nuclear export signal

NLS Nuclear Localization signal

NTBI Non-transferrin Bound Iron

PAI-1 plasminogen activator inhibitor -1

PCC Pearson's overlap correlation coefficient

PDK phosphoinositide-dependent protein kinase

PFA Paraformaldehyde

PKC Protein kinase C

PI3K phosphotidylinositol-3-kinase

PPAR Peroxisome proliferator-activated receptors

PVDF Polyvinylidene fluoride

ROS Reactive oxygen species

SDS-PAGE Sodium dodecyl sulfate polyacrylamide gel electrophoresis

Ser Serine

SOCS3 Suppressor of Cytokine Signaling 3

SOD2 Superoxide dismutase 2

T2D Type 2 Diabetes mellitus

TF Transcription factor

TfR1/2 Transferrin receptor protein 1/2

Thr Threonine

TNFα Tumor necrosis factor α

WHO World health organization

Chapter 1: Introduction and Research Aims

1.1 Metabolic Syndrome

The rapid progression of technology has facilitated the low cost and wide-spread production of high caloric foods in addition to the availability of jobs and activities that promote a sedentary lifestyle. It is, therefore, no surprise that global rates of metabolic-related diseases have been on the dramatic rise. According to a report published by the World Health Organization (WHO), of the 41 million deaths attributed to noncommunicable diseases in 2016, approximately half (19.5 million) of those were due to a combination of cardiovascular diseases and diabetes [1]. Cardiovascular diseases, according to the WHO, is considered to be the primary cause of death globally representing approximately 31% of all deaths [2]. Global obesity cases have reportedly tripled since 1975 with over 1.9 billion adults considered overweight and over 650 million considered obese [3].

The term "Metabolic Syndrome" (MetS) also otherwise referred to as "Syndrome X", "the insulin resistance syndrome" and "the deadly quartet" is an umbrella term used to describe a collection of diseases that increase the relative risk and contribute towards the development of cardiovascular diseases and Type 2 Diabetes Mellitus (T2D) [4]. The purpose of this unifying term was to aid in the clinical diagnosis of patients as well as to serve as a helpful research tool. MetS was coined by three separate bodies; a consultation group from the WHO, the National Cholesterol Education Program's Adult Treatment Panel III (NCEP:ATP III) and the European Group for the Study of Insulin Resistance [4]. While these three bodies may have subtle differences in their criteria for what constitutes MetS, their definitions revolve around the same five collection of physiological risk factors. These include: visceral obesity, elevated triglycerides, hypertension, high LDL - low HDL and elevated fasting glucose levels [4]. According to the International Diabetes Federation (IDF), MetS is officially defined as an individual who's symptoms must include visceral obesity and any two of five remaining conditions [5].

The challenge with developing such a definition was its applicability to a worldwide population. For instance, obesity can be determined by measuring the Body Mass Index (BMI). It was previously established that any value equal or greater than 30kg/m^2 was considered obese [5]. However, this value applied mainly to Western and Caribbean populations would not be applicable to Asian populations since the cut off values would be lower [5,6]. To circumvent this issue, visceral obesity was the criteria chosen, which was determined by abdominal waist circumference [7,80]. This measure was easily quantifiable by clinicians and better accounted for ethnic differences when referenced to established population-specific values. The following data obtained from a meeting that included several major bodies determined that abdominal obesity would be defined as a waist circumference greater or equal to 94 cm and 80 cm in men and women respectively [8].

Visceral or abdominal obesity is considered a risk factor due to its proclivity to induce a state of insulin resistance caused by several factors such as the presence high amounts of non-esterified fatty acids (NEFA) [7,81]. It is has been shown that with the increase in visceral adipose tissue, due to adipocyte hypertrophy, a change in the secretory profiles of adipokines is observed as summarized in figure 1.1. These include increases in leptin, interleukin 6, tumour necrosis factor alpha (TNF-α), C-Reactive Protein (CRP), resistin, angiotensinogen and plasminogen activator inhibitor -1 (PAI-1) in addition to decreases in adiponectin [7,9]. These changes result in increased free fatty acids (FFA) and elevated triglyceride content in adipocytes that ultimately induces a series of changes in a variety of organs that all feed into the T2D pathology. These include an ectopic accumulation of fat in the liver leading to impaired liver function and increased hepatic gluconeogenesis, a compensatory reaction by pancreatic beta cells in response to insulin resistance resulting in hyperinsulinaemia and impaired glucose uptake in skeletal muscle [7,81]. Adiponectin, of particular interest, diverts from the trend of increased levels of adipokines and typically functions as an insulin-sensitizing, anti-inflammatory, anti-

3

atherogenic hormone [9, 10]. Its decrease, therefore, contributes to a hyperglycemic state via impaired glucose uptake and further exacerbates elevated triglyceride levels due to impaired fatty acid oxidation [9,10].
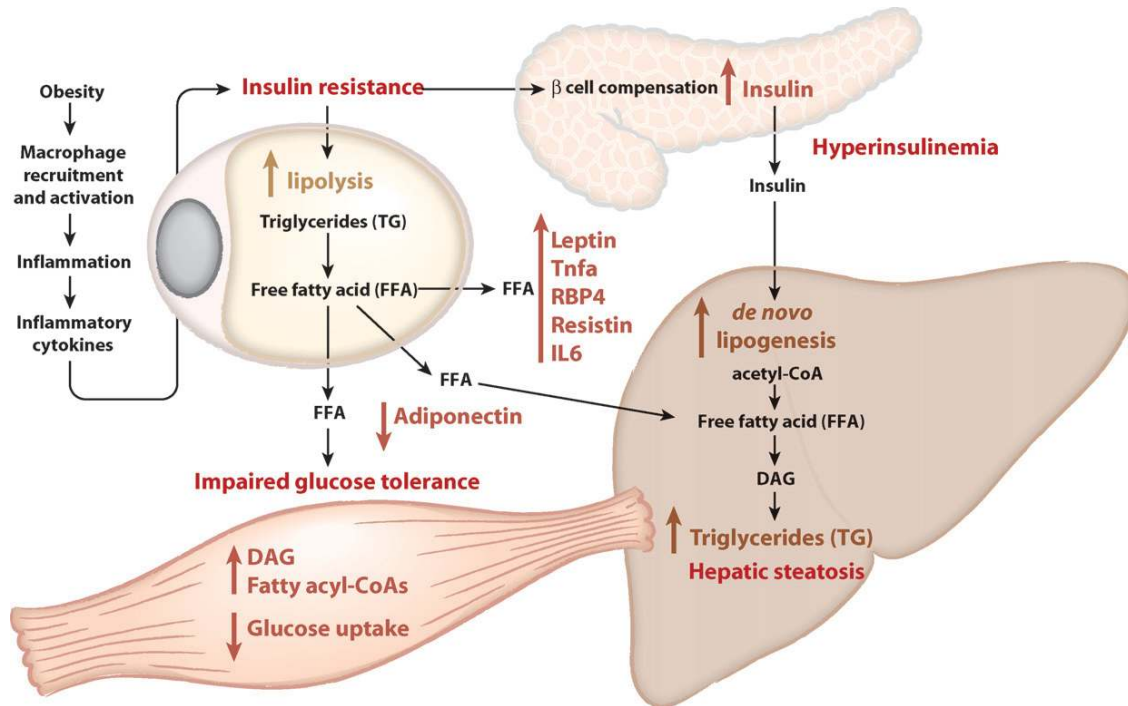
Figure 1.1: Schematic highlighting the effects of obesity, how insulin resistance and T2D arise at sites such as adipose tissue, pancreas, liver and skeletal muscle [9]. Image taken from Attie, A. D., & Scherer, P. E. (2009). Adipocyte metabolism and obesity. *Journal of lipid research*, *50*(Supplement), S395-S399

1.2 Type 2 Diabetes mellitus

According to the WHO, the number individuals afflicted with diabetes has grown from 108 million in 1980 to 422 million in 2014 with 1.6 million deaths attributed directly to diabetes in 2016 [11]. In addition, according to the International Diabetes Federation (IDF), Type 2 Diabetes mellitus (T2D) has been shown to affect nearly 8% of the world's adult population and has been projected that a 55% increase in T2D incidence rates will occur within the next 20 years leading to a total of 592 million people being afflicted with the disease worldwide [12,13]. With T2D's meteoric rise to pandemic levels, much ground needs to be covered with regards to its etiology.

4

T2D, also referred to as insulin resistance, is typically characterized by hyperglycemia caused by impaired insulin signaling due to a number of reasons. These include a reduction in the amount of circulating insulin produced by pancreatic beta cells, a reduction in the number of insulin receptors available or an impairment in the downstream signaling [13]. Pancreatic beta cell hyperplasia and hyperinsulinemia are thought to occur prior to the onset of diabetes in a state called "pre-diabetes" [13].

T2D is considered to be the central figure in MetS pathology and many of the risk factors associated with MetS lead to the development of insulin resistance [10,14]. In insulin-sensitive individuals, insulin exerts its effect by binding to its insulin receptor (IR), typically found in glucose utilizing organs such as skeletal muscle and liver (figure 1.2). Upon binding, the intracellular IR beta subunit tyrosine kinase is activated leading to autophosphorylation of the insulin receptor and its substrates: insulin receptor substrate 1 and 2 (IRS-1,2) [15,16]. Once phosphorylated, IRS-1 activates the regulatory subunit of phosphotidylinositol-3-kinase (PI3K) which leads to the activation of phosphoinositide-dependent protein kinase (PDK) and in turn, either/or Akt and protein kinase C (PKC) [16]. The activation of Akt and PKC leads to the translocation of a glucose transporter, GLUT4 in the case of skeletal muscle, to facilitate glucose uptake as well as the suppression of hepatic gluconeogenesis [16,17].
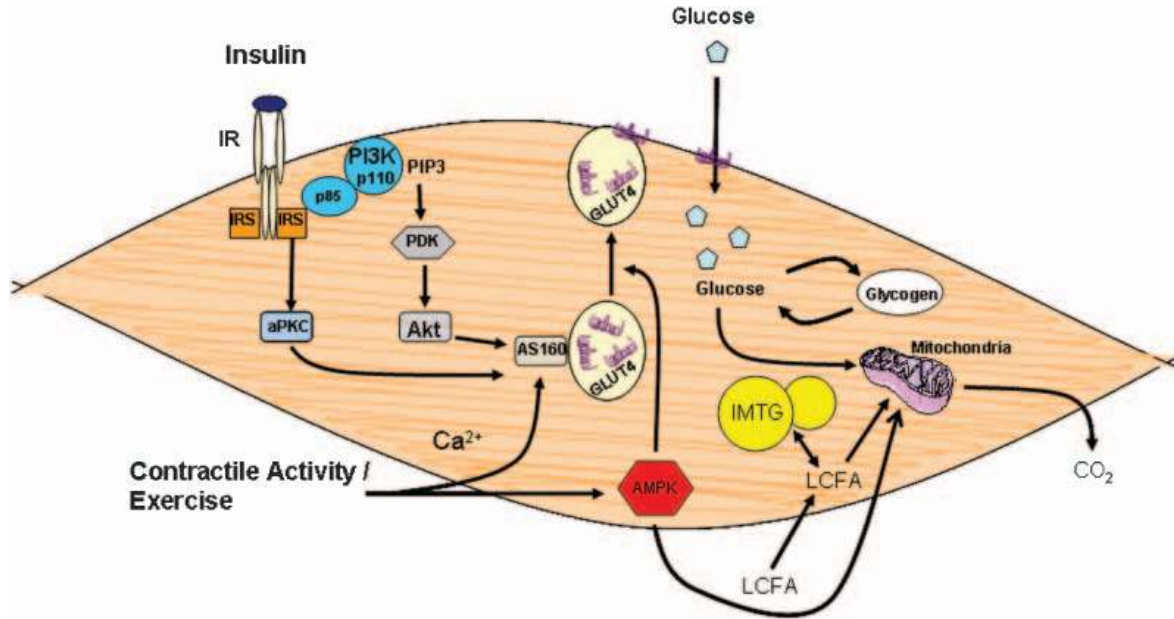
Figure 1.2: Summary of the insulin signaling pathway in skeletal muscle [16]. Image taken from Stump, C. S., Henriksen, E. J., Wei, Y., & Sowers, J. R. (2006). The metabolic syndrome: role of skeletal muscle metabolism. *Annals of medicine*, *38*(6), 389-402.

In cases of insulin resistance, a number of mechanisms have been brought forth to explain the pathology. One prevailing mechanism which involves the effects of other MetS risk factors such as visceral obesity and elevated triglycerides are the effects of inflammatory cytokines and accumulation of free fatty acids. In the case of visceral obesity, as previously mentioned, several pro-inflammatory cytokines including TNF-α and C Reactive Protein (CRP) secreted from adipocytes can activate serine/threonine kinases such as c-Jun N-terminal Kinase (JNK) which inhibit insulin action by phosphorylating serine/threonine residues on IRS-1 thus inactivating both PI3K and Akt leading to decreased glucose transporter translocation [13,16,18]. With regards to elevated free fatty acids, these result in increased diacylglycerol, which can result in activated alternative isoforms of PKC leading to the activation of both JNK and NF-kB pathways [13]. Free fatty acids have also been reported to increase hepatic gluconeogenesis thereby further promoting a hyperglycemic state [18].

6

1.3 Iron: Role and significance in metabolic diseases

1.3.1 Importance of iron and iron regulation

Iron is a divalent metal that is involved in a wide range of vital cellular processes such as oxygen transport in hemoglobin, DNA synthesis, oxidative phosphorylation and cellular immune responses [19,20]. Iron can exist in either the ferric (Fe^{3+}) or ferrous (Fe^{2+}) form and it is these dual forms that facilitate its involvement in oxidation/reduction reactions [20,21]. Iron is typically obtained through dietary means that can be divided into heme and non-heme sources [22]. Heme sources comprise of iron found in hemoglobin and myoglobin from animal products such as red meat while non-heme sources include fortified cereals, vegetables and beans [22]. Other sources of iron include parenteral iron, inhaled iron and recycled iron ions from the erythroid pool generated from endocytosed erythrocytes [21,22,23].

Since mammals do not have a specialized excretory system dedicated to iron, its regulation is of utmost importance. In the case of dietary iron, ferric iron is reduced to ferrous iron in the small intestine by the ferrireductase duodenal cytochrome B (DCTB) (Figure 1.3). The ions proceed to enter the duodenal enterocytes via divalent metal transporter 1 (DMT1). Fe^{2+} exits the enterocytes through iron export channel ferroportin and is oxidized into Fe^{3+} by hephaestin where it immediately binds to transferrin in circulation [20,21]. Iron bound transferrin (TBI) can be internalized by binding to one of its two receptors: transferrin receptor-1,2(TfR1,2) or can remain soluble in the circulation [20,21]. Soluble iron bound transferrin-transferrin receptor can be used as a biomarker to evaluate functional iron deficiency [20,21]. Most cells exhibit TfR1 and upon binding of iron bound transferrin to its receptor, the complex is internalized and Fe^{3+} is released from transferrin, reduced by the STEAP family of ferrireductase to Fe^{2+} and enters the cytosol through DMT1 [20,21]. Another form of iron to consider with regards to entry is non-transferrin bound iron (NTBI). Once transferrin levels reach saturation, such as in cases of IO, the excess iron circulates as NTBI [100,101]. While the precise mechanisms of NTBI internalization are still debated,

there several proposed mechanisms behind how this occurs. These mechanisms typically involve ferrireductases such as the previously described DCTB that is found bound on the cell surface as well as other cellular reductants such as ascorbate, STEAP and cytochrome b561 [101,102]. The function of these enzymes is to convert ferric NTBI into the ferrous form, following which internalization is facilitated either via DMTs such as DMT1 or ZRT/IRT-like proteins (ZIPs) such as ZIP14 or ZIP8 [101,102].

Once in the cytosol, iron is regulated through the interaction with iron response elements (IRE) found on the mRNA of TfR1 and ferritin resulting in the release of iron response proteins (IRP). The interaction between iron and IRE on TfR1 mRNA results in decreased stability of TfR1 mRNA leading to decreased iron uptake. Iron interacting with the IRE on ferritin mRNA results in increased translation of ferritin which is most commonly used biomarker for deterring total body iron stores [20,21]. Iron-bound transferrin can also bind to TfR2, mainly found in the liver, and initiates the production of hepcidin [21]. Once produced, hepcidin plays a pivotal role in iron regulation by inducing the internalization and degradation of intestinal ferroportin thereby reducing iron absorption [21].
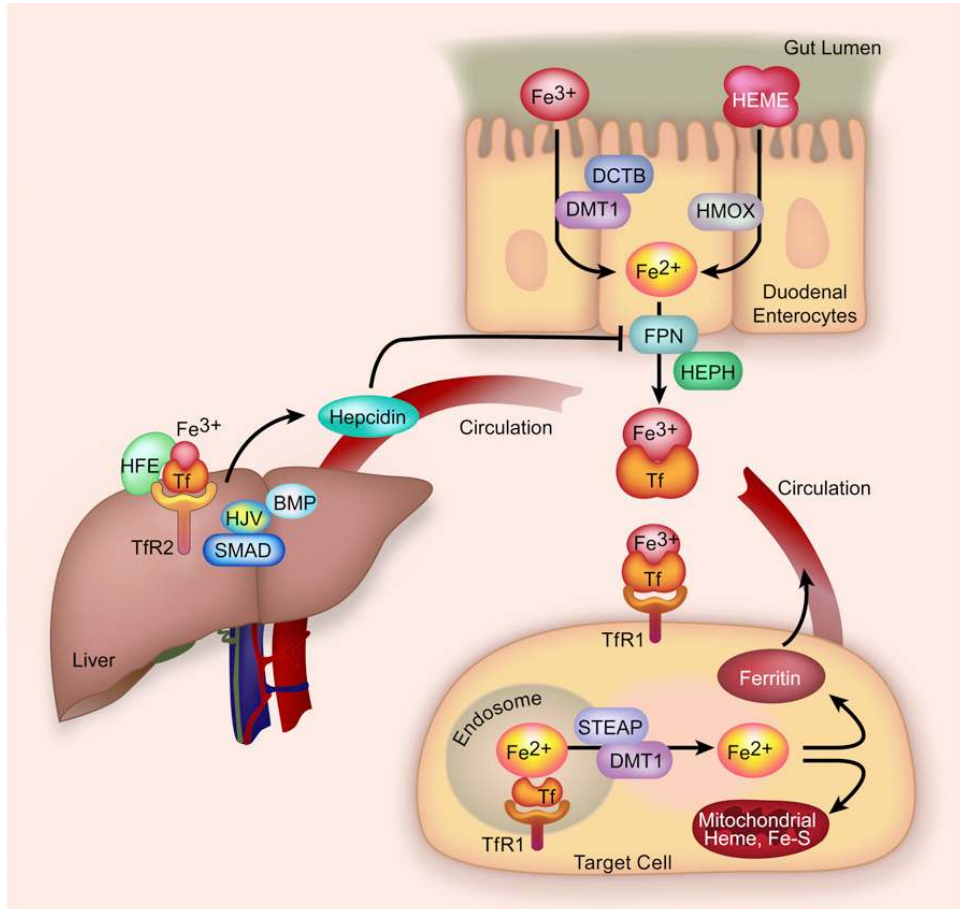
Figure 1.3: Summary of iron regulation [13]. **Image taken from Simcox, J. A., & McClain, D. A. (2013). Iron and diabetes risk.** *Cell metabolism*, *17*(3), 329-341.

1.3.2 Iron overload (IO) and related disorders

As described previously, clinicians and researchers typically use ferritin as the biomarker for total body iron stores. In healthy individuals, a total circulating iron content of 3-4g is observed. With regards to serum ferritin levels, healthy men and women exhibit a range of 12-300 ng/mL and 10-150 ng/mL respectively [21,22]. A state of iron overload (IO) is characterized by serum ferritin levels exceeding that of 300 ng/mL in men and 150 ng/mL in women.

Some of the more common pathological manifestations of IO include the genetic disorder Hereditary Hemochromatosis (HH) and beta thalassemia. HH is an autosomal recessive disorder that is found to occur in approximately 0.5% of Caucasian populations [21,22,23]. HH is characterized by a missense mutation that occurs on loci C282Y and H63D. These loci code for IRPs such as HFE protein which is required for hepcidin stimulation [19,21]. Other rarer mutations that occur on IRP but are still associated with HH include TfR2, hemojuvelin (HJV), hepcidin and ferroportin mutations [19,21]. The effects of these mutations collectively lead to the same outcome: increased iron absorption from the gut and into circulation due to impacted hepcidin levels resulting in IO. Beta thalassemia is a disorder characterized by an impairment in in the beta globulin subunit of hemoglobin [21,23]. This leads to the inability to produce functioning erythrocytes resulting in anemia. Thalassemic patients, therefore, are treated with regular blood transfusions which greatly overloads them with iron due to the increased labile plasma iron pool [21,23]. This is attributed to the fact that one unit of blood approximately 0.2 g of iron, or almost 100 times the amount of iron that is absorbed through the gut daily [21,23].

1.3.3 Significance of iron in MetS and T2D

In a survey conducted by the National Health and Nutrition Education Survey (NHANES) in the US, an increased risk of developing diabetes was observed in both men and women exhibiting elevated serum ferritin levels [21,25]. In addition to this finding, a later survey by the same group (NHANES III) revealed that the risk of developing MetS approximately doubled with increasing ferritin levels [21,26]. In one study where premenopausal woman (n=1645), postmenopausal women (n=1424) and men (n=2880) were examined (iron levels were lower than predefined IO levels) it was determined that the prevalence of elevated blood pressure, elevated plasma glucose, elevated triglycerides and visceral adiposity were all greatest in individuals at the highest quartile of circulating ferritin levels [26]. These findings were corroborated by several

other cross-sectional studies which confirmed the same association between elevated ferritin levels and several MetS risk factors including: hypertension [27], dyslipidemia [28], elevated fasting insulin and blood glucose [29] as well as visceral obesity [30]. Insulin resistance was additionally observed in postmenopausal women and men at higher ferritin levels as indicated by elevated fasting insulin and triglycerides [26]. Finally, an investigation conducted by the Epidemiological Study on the Insulin Resistance Syndrome (DESIR) revealed that high levels of both ferritin and transferrin were associated with increased prevalence of MetS at both the commencement of the study as well as after a 6 year follow up [22].

With regards to IO-based pathological conditions in relation to T2D, there have been numerous studies highlighting iron's causal role. In HH, ferritin levels are typically in the range of 1,000 to 10,000 ng/mL and approximately 25-65% of those afflicted exhibit symptoms of secondary T2D such as insulin resistance and glucose intolerance [22]. However, these symptoms have also been attributed to beta cell failure [22]. It is also worth noting that a significant majority of individuals afflicted with HH whom exhibited T2D were also classified as obese [21]. When considering individuals afflicted with beta thalassemia, incidence rates of T2D were observed at 6%-14% and typically displayed symptoms of insulin resistance rather than insulin deficiency [21]. This was thought to be due to the organs targeted by iron accumulation due to the differential hepcidin expression profile between HH and beta thalassemia [21]. When iron chelation therapy was administered, such as Deferoxamine or phlebotomy therapy, individuals exhibited significantly improved glucose tolerance and insulin sensitivity thus further substantiating iron's causal role in the development of T2D and other MetS morbidities [21,22].

Another important pathology when considering iron overload is Dysmetabolic Iron Overload Syndrome (DIOS). While individuals afflicted with DIOS do not exhibit the same high degree of circulating ferritin levels seen with HH or thalassemic patients, DIOS patients exhibit what is known as hyperferritnemia [32]. This state is characterized by a mild increase in hepatic

11

and body iron stores (indicated by either serum ferritin or transferrin) in addition to either a single or collection of MetS symptoms such as dyslipidemia, glucose intolerance, hypertension and steatohepatitis [32]. Individuals afflicted with DIOS have displayed increased iron localization in visceral adipose tissue as evidenced by increased hepcidin mRNA and decreased TfR1 expression [32]. It has also been reported that DIOS patients are at greater risk for developing MetS due to a differential secretory profile of adipokines due to iron loading. Studies performed on C57Bl/6 mice using iron supplemented diets to induce IO revealed increased hepatic and adipocyte iron accumulation, a fivefold increase in serum hepcidin levels, increased resistin, decreased serum adiponectin and leptin levels [32]. In addition to these findings, the study revealed a 40% increase in fasting glucose levels, which the researchers attributed to insulin resistance due to decreased insulin signaling and a threefold elevation in triglycerides [32,33].

1.3.4 Iron's role in T2D: Oxidative stress

The precise mechanism with which iron exerts its effect is a topic that is still currently debated. The general consensus is that iron exerts a multifactorial effect by targeting a collection of different processes at different sites that ultimately contribute to insulin resistance. Examples include increased hepatic iron stores which have been shown to induce insulin resistance by impeding suppression of hepatic gluconeogenesis via reduced insulin clearance [24]. Adipocyte iron loading, as previously discussed, has been shown to increase circulating resistin levels which has been reported to induce Suppressor of Cytokine Signaling 3 (SOCS3), an insulin signaling inhibitor [33,34]. Another example is pancreatic beta cell dysfunction due to iron loading. Pancreatic beta cells express divalent metal transporters that predisposes them to overloading with iron leading to decreased insulin synthesis and secretion [24].

The mechanistic theory that has gained most traction, mainly due to the abundance of evidence presented, is iron's proclivity to induce a state of oxidative stress. Iron is a pro-oxidant

12

and has been shown to induce the production of ROS through two main processes. The first involves iron acting as a catalyst in the Haber - Weiss/Fenton reaction where ferric iron is reduced, converting a superoxide radical ($\cdot O_2^-$) into O_2. The Fenton portion of the reaction occurs when ferrous iron reacts with hydrogen peroxide to produce a hydroxyl radical ($\cdot OH$) [35]. The generation of the hydroxyl radical is a primary source of oxidative stress that typically causes DNA, lipid, protein and cellular organelle damage [35]. The second process is irons involvement as a cofactor in electron transport chain (ETC) to generate ATP in the mitochondria [22,36]. Iron transfers electrons to oxygen at Complexes I,II and III of the ETC leading to the generation of the previously mentioned superoxide [35].

Instances of IO have been linked to decreases in antioxidant defence enzymes such as superoxide dismutase 2 (SOD2) and catalase indicating elevated oxidative stress [21]. When examining beta thalassemic patients, it was reported that elevated serum ferritin levels were linked to F2-isoprostanes, a marker for oxidative stress, as well decreased SOD [24]. Another contributing factor to pancreatic beta cell failure is the lack of antioxidant defenses present. Since pancreatic beta cells experience increased iron loading due to the presence of divalent ion channels, it has been reported that the lack of antioxidant enzymes further predisposes them to damage due to oxidative stress [21]. In addition, there have been findings suggesting that pancreatic beta cell dysfunction due to ROS could be attributed to a decrease in the transcription factors required for beta cell differentiation, proliferation and insulin gene transcription [21]. In other cases, ROS has been attributed to impaired insulin binding sensitivity due to hydroxylation of phenylalanine resides on insulin [21]. Finally, ROS have been shown to activate inflammatory specific kinases such as JNK, which as previously mentioned, has the capacity to activate PKC isoforms and result in the impairment of insulin signaling [13,35].

13

1.4 Adiponectin

1.4.1 Structure and regulation

Adiponectin is a 30 kDa adipokine from the complement 1q (c1q) family and is secreted by adipocytes who's main site of action include adipose tissue, skeletal muscle and the liver [36,38]. Adiponectin is encoded by *AdipoQ* that is found on chromosome 3q27, a loci of chromosomes shown to be particularly susceptible in instances of diabetes and cardiovascular diseases [38]. Gene expression of adiponectin is regulated by a variety of transcription factors including peroxisome proliferator activator receptor γ (PPAR-γ), C/EBPa, CREB and Forkhead transcription factor 1 (FOXO1) [38].

Adiponectin's structure is comprised of a carboxyl-terminal globular domain and an N-terminal collagen domain that resembles the c1q family of proteins that form multimers [37]. The formation of the multimer complexes is facilitated via a cysteine residue on the N-terminal collagen domain [37,40]. Adiponectin exists in 3 forms found in circulation: the trimeric low molecular weight form (LMW) which represents the most basic unit, a hexamer form deemed as the middle molecular weight (MMW) and the high molecular weight (HMW) also referred to as full length adiponectin (fAd) which is comprised of several hexamer subunits [37]. Post translational modifications (PTM) of adiponectin are crucial to its multimerization [41]. These PTMs include hydroxylation and glycosylation of lysine resides found on its N-terminal domain [41]. fAd can be cleaved to generate a 17 kDa globular adiponectin (gAd), albeit circulating levels are very low compared to fAd (2-30µg/mL) [38,39]. Studies have demonstrated that the HMW form of fAd has been shown to exerts its pleiotropic effects. These include, but are not limited to anti-diabetic, anti-atherogenic, anti-inflammatory and anti-fibrotic effects [36,37,38].

Finally, secretion of adiponectin is regulated by chaperones originating in the endoplasmic reticulum (ER) including ERp44, ER oxidoreductase -1La (Ero-1La) and disulfide bond A oxidoreductase-like protein (DsbA-L) [41]. ERp44 plays an inhibitory role by limiting the

14

release of adiponectin from the ER via the formation of a disulfide bond with its variable region. Ero-1La functions to release adiponectin from the ER by displacing adiponectin from its interaction with ERp44. DsbA-L has been shown to act as a disulfide isomerase that regulates the formation of disulfide bonds between adiponectin monomers during multimerization [40,41].
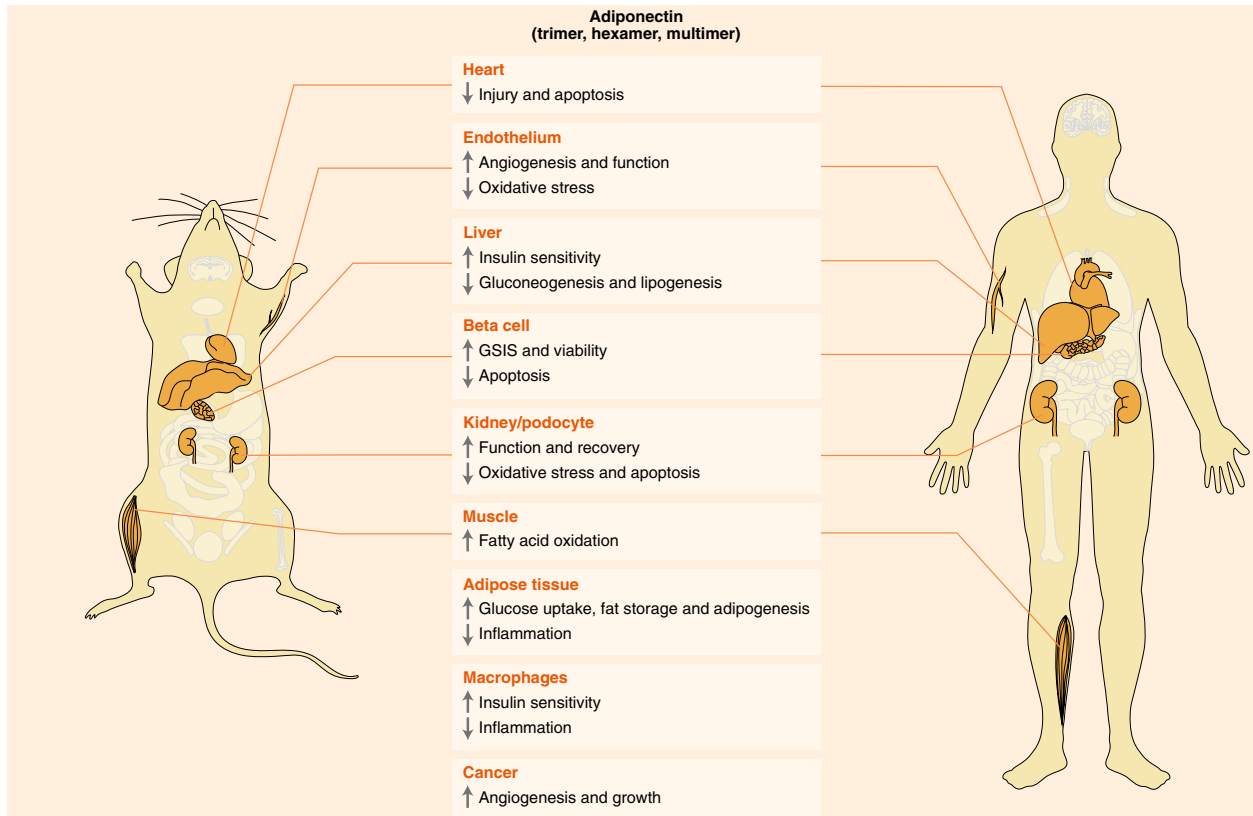
Figure 1.4: Overview of the broad range of effects adiponectin has in variety of target organs/tissues [82]. Image taken from Straub, L. G., & Scherer, P. E. (2019). Metabolic Messengers: adiponectin. *Nature Metabolism, 1*(3), 334

1.4.2 Adiponectin signaling proteins

Adiponectin exerts its effects by binding to one of its primary receptors: Adiponectin receptors 1 or 2 (AdipoR1/2). AdipoR1/R2 are encoded by genes found on chromosomal regions 1p36.13-q41 and 12p13.31 respectively [41]. These proteins are members of the PAQR family of receptors and are structurally similar to GPCRs but functionally distinct [42]. They are made up of

a seven transmembrane domain with inverted topology where the C terminus (approximately 25 amino acids) is found on the extracellular surface and the N terminus on interior [38,41,42]. It has been reported that AdipoR1 is ubiquitously expressed in all tissues, however, a larger portion is typically found in skeletal muscle while AdipoR2 is mostly found in the liver [41]. Furthermore, studies have reported that the two adiponectin receptors express different affinities to specific forms of adiponectin with AdipoR1 favouring gAd and AdipoR2 favouring fAd [41].

T-Cadherin, a glycolsylphosphatidylinositol-anchored protein, is a third receptor that adiponectin has been shown to interact with [42]. T-cadherin has been reported to have affinities to the MMW and HMW forms of adiponectin and is primarily located in the heart, smooth muscle and endothelium [38,40]. T-cadherin is required for adiponectin to exert its cardioprotective effects, however, it is not a typical receptor due to the absence of any intracellular signalling or cytoplasmic components [40]. The mechanism behind how T-cadherin facilitates adiponectin action requires further study.

Upon successful binding of adiponectin to one of its primary receptors (AdipoR1/AdipoR2), an adaptor protein known as the adaptor protein containing pleckstrin homology domain, phosphotyrosine binding domain and leucine zipper motif (APPL1) is activated [43]. As its name suggests, APPL1 is made up of different regions each with vital roles in facilitating adiponectin signaling. The leucine domain, also referred to by some as the BAR (NH2-terminal Bin 1/ ampliphysin / rvs167) domain, is responsible for membrane curvature induction, small GTPase binding, transcriptional repression, apoptosis, and secretory vesicle fusion [41]. The pleckstrin homology (PH) directs proteins to specific membrane compartments by increasing lipid specificity of the BAR region [41]. The phosphotyrosine binding domain (PTB) is responsible for scaffolding proteins destined to interact with APPL1 [41]. Another adaptor protein (APPL2) is also found to interact with AdipoR1/AdipoR2. APPL2 exhibits approximately 54% homology to

16

APPL1 [41,42]. It has been reported that that APPL2 can bind to APPL1, via the BAR region, preventing any interaction with AdipoR1, thus impairing adiponectin signaling [42].

1.4.3 Adiponectin function and effector proteins

As mentioned previously, adiponectin has been shown to act as an anti-diabetic, anti-atherogenic, anti-inflammatory and anti-fibrotic compound [36,37,38]. These effects are facilitated via activation of adiponectin's effector proteins. These include: AMP-activated protein kinase (AMPK), acetyl-CoA carboxylase (ACC), peroxisome-proliferator-activated receptor alpha (PPAR- α), and P38 Mitogen Activated Protein Kinase (P38 MAPK) [43]. APPL1 has been demonstrated to play a vital role in mediating adiponectin function via overexpression and knockout approaches. Overexpression of APPL1 in skeletal muscle cells resulted in increased phosphorylation and activation of AMPK and P38 MAPK while APPL1 knockout resulted in decreased adiponectin stimulated phosphorylation of AMPK, P38 MAPK, ACC and decreased fatty acid oxidation [43,44]. With regards to adiponectin's insulin sensitizing effect, studies have emerged uncovering a cross-talk occurring between APPL1 and IRS-1/2 [43]. Initially, it was determined that upon APPL1 KO in C2C12 myotubes, insulin stimulated Akt phosphorylation was significantly impaired [43,44]. Overexpression of APPL1 resulted in enhanced insulin stimulated Akt activation [43,44]. It is also worth noting that administration of adiponectin alone had no effect on Akt phosphorylation and that the observed activation of Akt was only detected upon co-administration of adiponectin and insulin [43,44]. APPL1 Is thought to facilitate this cross-talk with AdipoR1 through a number of mechanisms. One such mechanism is the ability of APPL1 to form complexes with IRS1/2 under basal conditions [83]. Upon insulin or adiponectin stimulation, this complex is recruited to IRs and potentiates insulin signaling thus explaining adiponectin's synergistic effect on Akt phosphorylation [83]. Other suggested mechanisms include APPL1 interacting with the p110 catalytic subunit of PI3K and Akt [43,44].

17

It had been previously reported that gAd is the predominant form of adiponectin found to interact with AdipoR1 in skeletal muscle [43]. Several studies have demonstrated that adiponectin stimulated activation of AMPK results in increased glucose uptake and lactate production in skeletal muscle while also reducing expression of enzymes involved in gluconeogenesis such as phosphoenolpyruvate carboxykinase (PERK) and glucose-6-phosphotase (G6Pase) in the liver [40,44,45]. AMPK is typically phosphorylated by LKB1 as well as Ca^{2+}/calmodulin dependent protein kinase kinase (CaMKK) [42,46]. Adiponectin had been demonstrated to stimulate the translocation of LKB1 from the nucleus to the cytosol via APPL1 activation, resulting in the phosphorylation of AMPK [46]. In addition, adiponectin triggers the release of Ca^{2+} ions from the ER which stimulates the phosphorylation of AMPK via CaMKK [42]. Kadawaki et al showed that upon adiponectin mediated activation of AMPK, ACC is phosphorylated via AMPK and an increase in fatty acid oxidation is observed [40,44]. ACC is thought to increase fatty acid oxidation by facilitating the reduction of malonyl-CoA levels leading to decreased carnitine palmitoyltransferase 1 activity resulting in increased fatty acid oxidation [44]. Adiponectin stimulated activation of AMPK has also been reported to increase insulin sensitivity [43,44]. This effect involves two major players in the insulin signaling pathway: p70 S6 Kinase (S6K) and IRS-1. Activation of AMPK has been linked to increased tuberous sclerosis complex 2 (TSC2) activity resulting in decreased S6K activation [44]. Increased S6K activity is associated with decreased IRS-1 tyrosine phosphorylation, therefore, reduced activity S6K was found to increase insulin sensitivity [44]. Adiponectin mediated AMPK activation was additionally reported to decrease phosphorylation of IRS-1 at sites Ser^{302} and $Ser^{636/639}$ which are known to be inhibitory sites of insulin signalling [44].Peroxisome proliferator-activated receptor γ coactivator -1α (PGC-1α) has also been shown to be activated via adiponectin stimulated AMPK phosphorylation resulting in increased mitochondrial biogenesis [42].

18

Binding of adiponectin to AdipoR2 results in the activation of PPAR-α [36]. This transcription factor results in the elevated transcription of gene targets responsible for proteins such as acetyl CoA oxidase (ACO), uncoupling proteins (UCPs). The increase in expression of ACO and UCP results in elevated fatty acid oxidation, energy expenditure and decreased skeletal muscle triglyceride content [47,48].

Finally, adiponectin can also exert its function by manipulating circulating ceramide levels. Adiponectin has been shown to activate cellular ceramidase thereby lowering ceramide levels and increasing sphingosine-1-phosphate which results in improved insulin sensitivity [40,48].
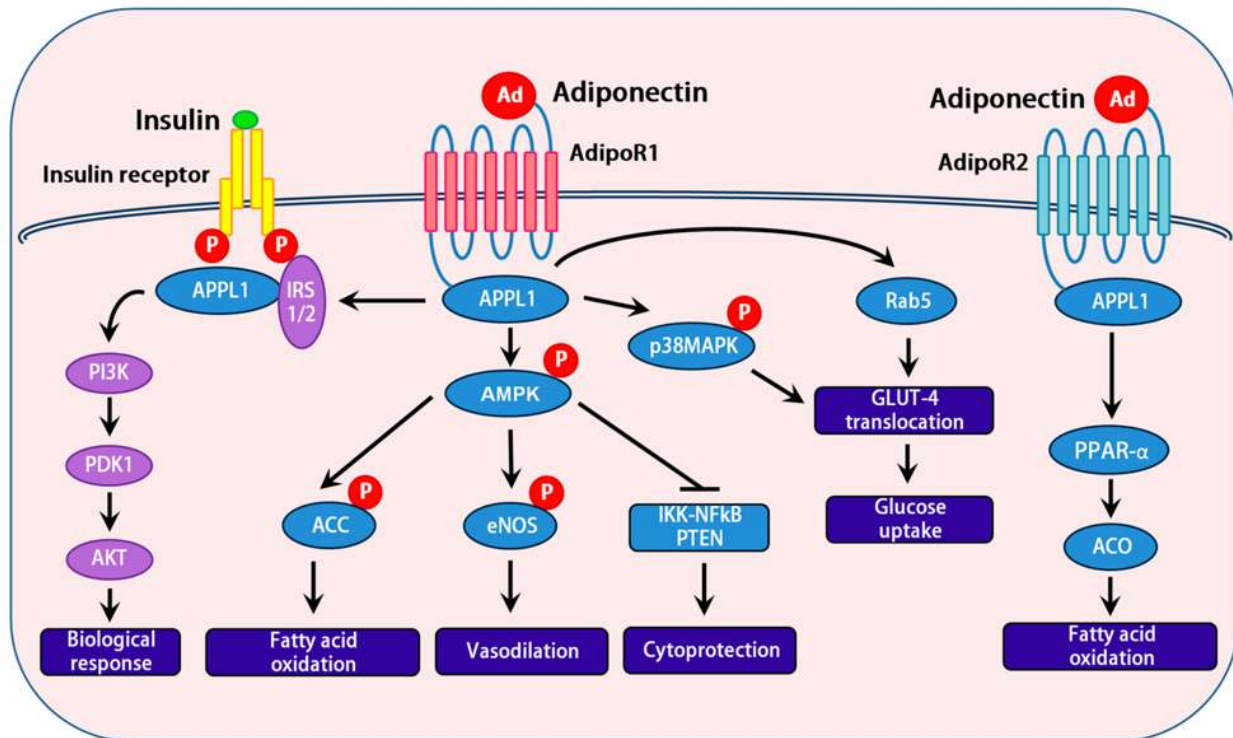

Figure 1.5: Overview of adiponectin signaling via AdipoR1/R2 and resulting effects [41]. Image taken from Achari, A., & Jain, S. (2017). Adiponectin, a therapeutic target for obesity, diabetes, and endothelial dysfunction. *International journal of molecular sciences, 18(6), 1321*

1.4.3.1 P38 MAPK

P38 MAPK is an effector protein that is activated upon binding of adiponectin to AdipoR1 in skeletal muscle [37,45]. P38 MAPK is a member of the mitogen activated protein kinases (MAPK) that regulates several cellular functions including inflammation, cell differentiation, cell growth and cell death [43]. The MAPK family is known to function as an intracellular signaling pathway that responds to extracellular stimuli. Four subgroups exist in the MAPK family which include the Extracellular signal-regulated Kinases (ERK), c-jun-N terminal or stress activated protein kinases (JNK/SAPK), ERK/big MAP kinase1 (BMK1) and the P38 MAPKs [49]. P38 MAPK is characterized as a Thr-Gly-Tyr (TGY) dual phosphorylation motif and exists as four isoforms that share up to 60% homology among each other but only 40-45% homology with the other MAPKs [50,51]. The four isoforms are: $P38_\alpha$ that is found ubiquitously expressed in all cell types, $P38_\beta$ in the brain, $P38_\gamma$ in skeletal muscle and $P38_\delta$ in endocrine glands [50,51]. P38 MAPK has been reported to be activated and play a role in response to extracellular stimuli such as UV light, heat, osmotic shock, inflammatory cytokines such as TNF-α and Interleukin 1, as well as growth factors [49,50]. P38 MAPKs are also involved in apoptosis, where caspase (integral proteins involved in apoptosis) inhibitors have been reported to inhibit P38 MAPK activation [50]. This effect, however, has been shown to be cell and P38 isoform specific since other forms of P38 have been reported to activate cell survival, growth and differentiation processes [50]. It is therefore apparent that the multitude of different scenarios that activate P38s, localization in addition to the availability of four isoforms that react differently to each stimulus accurately reflects the sheer complexity of understanding this class of kinases.

With regards to adiponectin, it had been previously established that adiponectin stimulated activation of P38 MAPK results in increased glucose uptake and fatty acid oxidation [47,51,52]. Adiponectin mediated increase in fatty acid oxidation in C2C12 cells was shown to be facilitated via a sequential activation of AMPK followed by P38 MAPK which results in

20

phosphorylating and activating PPAR-α [47]. Furthermore, 5-aminoimidazole-4 caboxamide ribonucleoside (AICAR) stimulated cells exhibited increased glucose uptake via Glut4 and Glut1 as a result of both AMPK and P38 MAPK activation [52]. The primary kinases responsible for activating P38 MAPK include transforming growth factor-β-activated kinase 1 (TAK1), mitogen activated protein kinase kinase 3 (MKK3) and MKK6 [50,51]. However, it was determined that adiponectin stimulated APPL1 acts as a scaffold that facilitates P38 MAPK phosphorylation via activation of TAK1 and MKK3 only [52].

1.4.4 FOXO1: Role in adiponectin receptor expression

The Forkhead Box "Other" family of transcription factors (TFs) have been implicated in many vital cellular processes. These include, but not limited to, cell cycle arrest, DNA repair, apoptosis, glucose metabolism, aging and autophagy [54]. The FOXO family consists of FOXO1, FOXO3a, FOXO4 and FOXO6 [54]. These TFs have been detected in skeletal muscle and are reported to be involved in processes such as regulation of muscle mass, muscle fiber type specificity and metabolic flexibility [55]. Since the FOXO family is involved in such a wide range of functions, its regulation is of utmost importance. FOXO TFs are regulated via post translational modifications (PTMs) that include phosphorylation, acetylation, ubiquitination, methylation and glycosylation [54]. The effect of these PTMs can manifest itself by either altering FOXO localization (nuclear vs cytosolic), modifying half-life and DNA binding capabilities [54].

Phosphorylation of FOXO has been reportedly facilitated by variety of kinases, most notable of which include: Akt/Protein Kinase B, mammalian Ste20-like kinase (MST1) and JNK, P38 MAPK, cyclin dependent kinases (CDKs), AMPK, and Ikappa B kinase (I_kK) [54]. In general, phosphorylation of FOXO initiates the nuclear extrusion of FOXO resulting in decreased transcriptional activity [54]. This can be attributed to a number of mechanisms such as binding of the chaperone protein 14-3-3 which alters the structure of the nuclear localization signal (NLS)

21

on FOXO enhancing its extrusion as well as the induction of a mutation in the nuclear export signal (NES) [54]. However, phosphorylation can also result in the increase of FOXO transcriptional activity, as evident by situations involving oxidative stress [54]. During instances of oxidative stress, MST1 is activated, leading to enhanced phosphorylation of the forkhead domain (FHD) on the FOXO TFs resulting in reduced interaction with 14-3-3 and increased nuclear localization [54,55]. JNK also plays role in phosphorylating FOXO4 under oxidative stress resulting in increased nuclear translocation and transcriptional activity [54,55]. It is therefore important to note that FOXO proteins can have contradictory effects, and these effects are heavily based on conditions and cell type.

In the case of acetylation, CBP/p300 has been reported to interact directly with FOXOs, increasing acetylation and resulting in attenuated transcriptional activity attributed to cytosolic translocation as well as impaired DNA binding capabilities [54]. Once acetylated, or phosphorylated, FOXO TFs are mono or polyubiquinated and destined for degradation via the ubiquitin proteasome pathway [56,57].

Finally, with regards to adiponectin receptor regulation, numerous studies have reported that FOXO1 plays a role in the expression of both adiponectin and AdipoR1/R2. It was initially determined that the expression of AdipoR1/R2 was downregulated in cases of increased insulin signaling [58,59]. Upon the use of a PI3K inhibitor, an integral protein in the insulin signaling pathway, the decrease in AdipoR1/R2 mRNA initially observed was reversed [58]. It therefore determined that PI3K activation of Akt, a known FOXO1 interacting kinase and downstream effector of PI3K, was responsible for phosphorylating FOXO1 and attenuating its transcription of AdipoR1/R2 genes [58].

1.4.5 Adiponectin resistance, T2D and oxidative stress

There are cases where a state of adiponectin resistance is observed in obese and diabetic individuals in spite of lowered circulating adiponectin levels. As mentioned previously, a hallmark symptom of obesity and T2D is increased visceral adiposity which has been shown to negatively correlate with circulating adiponectin levels [18]. The reduction in adiponectin resulting in decreased fatty acid oxidation and glucose uptake, in addition to the ectopic accumulation of fat in skeletal muscle leads to impaired insulin signaling resulting in insulin resistance and T2D [65]. In a landmark study conducted on isolated human skeletal muscle, researchers demonstrated that treatment of gAd resulted in an additive effect regarding insulin stimulated glucose uptake and fatty acid oxidation in both obese and lean subjects [67]. However, the researchers also inadvertently showed that this additive effect was blunted in obese individuals versus their control counterparts [67]. This suggests a phenomena of adiponectin resistance present in obesity. This finding was corroborated by the Kadawaki group that observed decreases in AdipoR1/R2 mRNA levels in the skeletal muscle and adipose tissue of insulin resistant, obese mice [37]. Kadawaki suggested that obesity was shown to decrease both circulating adiponectin and its receptors, reducing adiponectin signaling resulting in insulin resistance which is shown to induce hyperinsulinaemia [37]. The increase in circulating insulin could potentially be another mechanism to decrease adiponectin receptor expression via reduced FOXO1 transcriptional activity. It is important to note that adiponectin resistance has been shown to precede insulin resistance in a high fat diet (HFD) mouse model [65]. Adiponectin was shown to stimulate fatty acid oxidation and ACC phosphorylation in the control group but was significantly impaired in the HFD group in as early as 3 days [65]. Hallmark observations of insulin resistance including increased fatty acid transporters and increased DAG content resulting in impaired insulin signaling were observed approximately two weeks post HFD [65].

23

With regards to iron, as previously discussed, observations of increased serum ferritin levels correlated with decreased circulating adiponectin levels [63]. Furthermore, the McClain group additionally showed that AdipoR1/R2 mRNA levels in adipocytes was decreased by 30% in mice feeding on an iron supplemented diet [63]. This effect was attributed to increased deacetyation of FOXO1 which was shown to increased binding to PPAR response elements in conjunction with PPAR-γ resulting in repressed transcriptional activity [63]. While this explanation is rather convoluted, it is worth noting that iron's proclivity to induce a state of oxidative stress could potentially alter both kinase and acetylase activity responsible for FOXO PTMs. FOXO TFs are considered to be critical mediators of oxidative stress with several alterations in their PTM status occurring [57]. Examples include increased JNK and MST1 activity under oxidative stress resulting in increased nuclear translocation of FOXO4 and FOXO3 respectively [57]. Furthermore, increased transcriptional activity of FOXO3 under oxidative stress has been shown to increase expression of the anti-oxidant enzyme manganese superoxide dismutase (MnSOD) [57]. In conclusion, it is viable that iron induced oxidative stress could be a potential mechanism to explain the changes in FOXO1 transcriptional activity resulting in decreased expression of AdipoRs.

1.5: Hypotheses and research goals

1.5.1 Research goal 1: Establishing IO model in L6 skeletal muscle cells

An IO model was first established by conducting a series of experiments to determine the optimum dosage and time of IO exposure. To ensure the selected parameters induced a state of IO, the biomarker for total iron stores, ferritin, was investigated at both mRNA and protein level.

1.5.2 Hypothesis 1: IO induced adiponectin resistance

Once the experimental model was confirmed to be functional, adiponectin signaling was examined via P38 MAPK readout. Adiponectin receptors (AdipoR1/R2) as well as associated adiponectin proteins (APPL1/APPL2) were examined. The hypothesis was:

Treatment of L6 skeletal muscle cell with IO will result in adiponectin resistance.

1.5.3 Research goal 2: Monitor effect of IO on AdipoR transcription factor FOXO1

With AdipoR1 mRNA levels determined to decrease under IO, the next goal was to examine if IO had any effect on FOXO1. This would include PTMs as well as cellular localization.

1.5.4 Research goal 3: Characterize IO induced ROS production

To establish a mechanism pertaining to IO's effects on adiponectin signaling and FOXO1, iron's tendency to instil a state of oxidative stress was explored. To do so, IO induced ROS production was investigated.

1.5.5 Hypothesis 2: Mechanistic role of IO induced ROS production on adiponectin signaling and FOXO1 PTM localization

After characterizing IO induced ROS production, oxidative stress was investigated to determine its role, if any, in inducing adiponectin resistance. The hypothesis was: *IO induced ROS production leads to increased cytosolic localization and reduced transcriptional activity of FOXO1, resulting in adiponectin resistance.*

Chapter 2: Iron overload reduces adiponectin receptor-1 expression via a ROS/FOXO1-dependent mechanism leading to adiponectin resistance in skeletal muscle cells

2.1 Abstract

Iron overload (IO) is a common yet underappreciated observation in metabolic syndrome (MetS) patients. With the prevalence of MetS continuing to rise, it is of utmost importance to further elucidate mechanisms leading to metabolic dysfunction. IO positively correlates with reduced circulating adiponectin levels yet the impact of IO on adiponectin action is unknown. Here, we established a model of IO in L6 skeletal muscle cells and found that it induced adiponectin resistance, measured by reduced P38 MAPK phosphorylation by the adiponectin receptor (AdipoR) agonist AdipoRon. This correlated with reduced mRNA and protein levels of AdipoR1 and its facilitative binding partner APPL1. IO caused phosphorylation, nuclear extrusion and inhibition of FOXO1, a known transcription factor for AdipoR1. Reactive oxygen species production was induced by IO and using NAC to prevent this attenuated the effect of IO in FOXO1 phosphorylation, localization and adiponectin resistance. In conclusion, our study identifies a ROS/FOXO1/AdipoR1 axis as a cause of skeletal muscle adiponectin resistance in response to IO. This new knowledge provides new insight on potential disease pathophysiology in MetS patients with IO.

27

2.2 Introduction

The metabolic syndrome (MetS) has a reported worldwide prevalence of up to 84% of the general population [4,80]. MetS is characterized by a collection of physiological risk factors that include visceral obesity, insulin resistance, hypertension and dyslipidemia [4,6,84]. These factors contribute to elevated risk of chronic metabolic disorders such as cardiovascular disease and type 2 diabetes (T2D). With the high global prevalence of MetS, new knowledge is continually needed to improve understanding of its etiology.

A recurring yet underappreciated research theme is the role of iron in MetS. In the majority of MetS cases elevated levels of iron have been consistently observed [20,60]. This has been demonstrated in numerous studies where increased serum ferritin levels, a biomarker for iron body stores, has positively correlated to increased incidence of T2D [20,60,85,86]. Indeed, iron chelation therapies, such as deferoxamine, have been shown to improve glucose tolerance thus, substantiating causal role of iron in metabolic disease [21]. Iron is involved in a wide range of vital cellular processes such as oxygen transport via haemoglobin and mitochondrial function [23]. Iron is also considered a pro-oxidant and serves as a co-factor for enzymes involved in redox reactions [20,23,87]. Iron overload (IO) leads to the generation of reactive oxygen species (ROS) which has been shown to have detrimental effects on tissues and cellular organelles [19]. Elevated levels of ROS have also been shown to negatively impact glucose uptake in muscle and fat as well as insulin secretion in pancreatic beta cells [21,61]. Thus, elevated oxidative stress is an established mechanism whereby iron induced cellular dysfunction.

Adiponectin exerts a range of beneficial therapeutic responses such as insulin sensitizing, anti-atherogenic, anti-inflammatory and anti-fibrotic effects [38,82]. Adiponectin-stimulated signaling pathways include P38 Mitogen Activated Protein Kinase (MAPK), AMP-activated protein kinase (AMPK) and peroxisome-proliferator-activated receptor alpha (PPAR-α) [47,62]. Studies have reported that adiponectin mediated activation of P38 MAPK results in glucose

transporter (GLUT)4 translocation to the plasma membrane in L6 myotubes, as well as activation of PPAR-α, resulting in increased fatty acid oxidation [47]. Interestingly, in T2D patients circulating adiponectin levels were inversely correlated to serum ferritin levels [63,88]. Adiponectin mRNA levels from adipocytes were also significantly decreased when mice were subjected to IO [63]. Thus, decreased adiponectin levels or reduced adiponectin signaling result in impaired insulin signalling and glucose intolerance in T2D.

FOXO1 is a transcription factor from the family of Forkhead box 'Other' proteins. This family of proteins is involved in multiple processes such as cell cycle arrest, DNA repair, apoptosis, glucose metabolism, aging and autophagy [55,89]. The FOXO family of transcription factors have been reported to exert their effects on gene expression via direct binding to DNA targets as well as through protein-protein interactions with other transcription factors [55]. These transcription factors are mainly regulated through post translational modifications (PTMs), most important of which include phosphorylation and acetylation [64,89]. Upon phosphorylation of FOXO1, the transcription factor is shuttled out of the nucleus and into the cytoplasm, effectively reducing its transcriptional capabilities [64]. Importantly, FOXO1 has been shown to stimulate the expression of the adiponectin receptor AdipoR1[64,90].

The purpose of this study was to examine the impact of IO upon adiponectin sensitivity. We established an IO model in L6 skeletal muscle cells and observed that these cells became adiponectin resistant. We also examined the mechanisms via which IO regulated alterations in adiponectin sensitivity and focused on ROS production, regulation of FOXO localization and activity and consequently AdipoR1 expression levels. The observations made are likely of great significance in adding to our knowledge of disease pathogenesis in MetS and in identifying when adiponectin-based therapeutics would be beneficial.

2.3 Materials and Methods

2.3.1 Cell Culture: Growth and maintenance of L6 skeletal muscle cell line

L6 skeletal muscle cells from *Rattus norvegicus* were used for all *in vitro* cell work. Cells were incubated at 37°C - 5% CO_2. L6 cells were grown in AMEM media containing 10% Fetal Bovine Serum (FBS) (Wisent Inc. #310-010-CL) and 1% antibiotic-antimycotic (Gibco Life technologies #15240-602). Cells were grown in 75cm^2 flasks (Falcon via VWR #353136) and were split at 70% confluency. To detach cells, 3ml of trypsin (Wisent Inc. #325-043) was added to the flasks which were placed in a 37°C-5% CO_2 incubator for 2 minutes. Flasks were gently tapped, and floating cells were collected and neutralized with 3ml of 10% FBS AMEM in a 15ml conical tube. Cells were spun down for 5 minutes at 2000 RPM and resuspended in 10ml of 10% FBS AMEM. 10% of total suspension was used for further culturing and plating. 0.5% FBS media was used to induce starvation prior to experimental treatment. IO treatment was previously optimized and established at 250μM- $FeCl_3$ (Sigma-Aldrich #451649). Increased adiponectin mediated signaling was achieved by treating cells with AdipoRon (AdipoGen® Life Sciences #AG-CR1-0156-M050), an adiponectin agonist, at 35μM for 30 minutes. Inhibition of ROS production was facilitated using the general ROS inhibitor N-Acetyl Cystine (NAC) (Sigma-Aldrich #A7250) at 500nM, 30 minutes prior to IO treatment.

2.3.2 Western Blot: Protein expression/phosphorylation profile determination of adiponectin receptors, associated proteins and FOXO1

Upon completion of treatment conditions, cells were collected from 6 well plates (Falcon #353046) using a stock Laemmli lysis buffer made up of Tris-HCl (pH 6.8, 0.5M) (BioRad #1610798), 10% SDS (ThermoFisher Scietific #15525017) , 7.5 mL glycerol (Sigma-Aldrich #G9012) and ddH2O. Working Laemmli buffer solution made up of 90% stock Laemmli lysis buffer and 10% beta-mercaptoethanol with the addition of a Pierce Protease/Phosphatase cocktail inhibitor (ThermoScientific #A32961). Samples were collected and centrifuged at 10,000

RPM for 10 minutes then denatured at 95°C for 5 minutes. Samples were either stored at -20°C or run on appropriately sized SDS-PAGE gel depending on target protein. Gel electrophoresis was conducted at ~105 V for 2h, followed by transfer to a nitro-cellulose membrane (BioRad #162-0177) at the same voltage for 1h. Membranes were blocked in 3% BSA (Bovine Serum Albumin) (Bioshop #ALB001.1) blocking solution for 1h, followed by incubation in primary antibody overnight. Primary antibody concentration used was generally a 1:1000 dilution unless specified otherwise in the results section. Secondary antibody used was an anti-rabbit igG horseradish peroxidase (HRP) conjugated antibody (Cell Signalling #7074) at 1:5000 dilution. Membranes were activated using Clarity Western ECL Substrate solution (Bio-RAD: #1705061) and visualized using X-ray film development techniques (GE Health Care via VWR #28906837). WB band intensity was quantified using ImageJ software, normalized to GAPDH (37kDa), βactin (45kDa) or α/β tubulin (52kDa) and compared to control.

AdipoR1 and AdipoR2 primary antibodies were kindly gifted from AstraZeneca (Sweden). APPL1 antibody was purchased from Antibody Immunoassay Services (AIS, Hong Kong). APPL2 antibody (#H00055 198-B01P) was obtained from Abnova. Ferritin Heavy chain primary antibody was obtained from Santa Cruz (#sc-376594), pFOXO1 (Ser256) primary antibody from cell signaling (#9461). pP38 MAPK (Thr180/Tyr182) and P38 MAPK were purchased from cell signaling (#9211 and #9212) respectively. GAPDH, βactin, α/β tubulin were obtained from cell signaling (#2118, #4970, #2144) respectively.

2.3.3 Analysis of intracellular iron levels using ferrozine assay

To determine iron content L6 cells were lysed with 200µl of a solution containing equal volumes of 1.4 M HCl and 4.5% (w/v) $KMnO_4$ in H_2O. Plates were sealed in aluminum foil and incubated at 60°C for 2h then 60µl of detection reagent (2.5 M ammonium acetate + 1 M ascorbic acid +

6.5 mM ferrozine + 6.5 mM Neocuproine) was added to each well followed by a further 30 minutes incubation at room temperature (RT). 280µl of mixture from each well was then transferred to a 96 well plate and the absorbance of each well measured at a wavelength of 550nm.

2.3.4 qPCR: Examining the effects of IO on mRNA expression of adiponectin receptors and associated proteins

In order to quantify relative mRNA values of proteins of interest, RT-PCR was conducted. mRNA sequences of interest were blasted on NCBI Primer BLAST and primers of interested were designed based on specifications best suited for maximal binding with SYBR Green. Primers tested are listed as follows:

	Forward (5' -> 3')	Reverse (3' -> 5')
AdR1:	ATATAAGGTCTGGGAGGGGC	CCAGTCAGGAAGCACATCGT
AdR2:	CAGAGCAGGAGTGTTCGTGG	ATTCCACTCAGACCCAAGCC
APPL1:	GAGTCCAACAATGAGGGGGA	CCCTACGATCCAGTTCAGCA
APPL2:	TGGTTCAGAGCATTCAGGTGG	TCCTGTTGATCTGCGGTGTG
FOXO1:	AGTTAGTGAGCAGGCAACAT	GGTGAAGGGCATCTTTGGAC
Ferritin (Light):	CCTACCTCTCTCTGGGCTTCTT	CGCTTCTCCTCGGCCAATTC
Ferritin (Heavy):	ATCATGACCACCGCGTCTC	AACAAGACATGGACAGATAGACGTA
18S:	CGTTGATTAAGTCCCTGCCCT	AGTCAAGTTCGACCGTCTTCT

Primers were designed to span exon-exon junctions and all possible transcript variants of the desired protein. 18S rRNA was used as the housekeeping gene required for data normalization. After treatment, cells were lysed and collected using TRIzol reagent (Thermofisher Scientific #15596026). Following collection of the lysates, phase separation was performed using a 5:1 TRIzol:Chloroform ratio. Samples were centrifuged at 12,000 RPM for 20 minutes at 4°C. Aqueous phase was removed and RNA isolation procedure was followed. 100% isopropanol (Sigma-Aldrich #I9516) was added in a 1:1 ratio and incubated at room temperature for 10

minutes. Samples were then centrifuged at 12,000 RPM for 15 minutes at 4°C. Samples proceeded to undergo RNA washing using 75% ethanol. Isolated RNA was quantified using Nanodrop. Reverse Transcription was performed with the use of a master mix comprising of: Reverse Transcriptase Buffer, Reverse Transcriptase, dNTP, Target Primer, RNAse Inhibitor, RNA and Nuclease Free water. Samples were heated at 42°C for 1h in a water bath, followed by 70°C for 5 minutes on a heat block. Samples were run on a thermal-cycler.

Data was quantified and analyzed using the delta delta Ct method.

2.3.5 ImmunoFluorescence: Analysis of effects of IO on P38 MAPK activation, pFOXO1 translocation and intracellular ROS production

Upon completion of the experimental treatment, multi-well containing coverslips were washed with PBS^{++} (1% Ca^{2+} and 1% Mg^{2+} fortified) buffer and fixed using a 4% paraformaldehyde (PFA) solution (Sigma-Aldrich #HT501128). If cell permeation was required, 0.1% TritonX100 was used as the permeating solution. Blocking was achieved using 3% BSA in PBS^{++}. Primary antibody concentration used was 1:500 unless otherwise specified. Alexa 546 goat anti-rabbit (# A-11035) was used as the secondary antibody at 1:1000. In order to stain the nuclei, a 3:1 ratio Prolong Antifade (Invitrogen #P36930) to Vectashield containing DAPI (Vectashield #H-1200) was used. Slides were visualized on a Nikon Confocal microscope. Nuclei were visualized on the DAPI channel while Alexa 546 was visualized on its namesake channel. In the case of CellROX Green (Molecular Probes by Life Technologies #C10422), 2.5µM was used for 30 minutes prior to fixation. CellROX Green was visualized via the FITC channel. Mean fluorescence intensities were detected and recorded for all cells in field of view via Nikon Elements Analyst software. Data was normalized relative to control. ImageJ plugin JACop was used to obtain Person Correlation Coefficient values of nuclear overlap of pFOXO1.

33

2.3.6 Plasmid Transfection/Dual Luciferase Reporter Assay: Assessment of AdipoR1 promoter and FOXO1 transcriptional activity

Adiponectin Receptor 1(AdR1)-Luciferase (generously provided by Dr. Myeong Ho Jung, Pusan National University [79]), FOXO-Luciferase, pGL3-Luciferase and Renilla reporter constructs (Generously donated by Dr. Tara Haas [91]) were used in a Dual Luciferase Reporter assays. Constructs were amplified and purified using the QIAGEN Plasmid Midi DNA Purification Kit (QIAGEN: Cat No: 12145). Constructs were sequenced following purification and used accordingly. AdR1-Luc/FOXO-Luc and Renilla -Luc construct were co-transfected into L6 cells using Lipofectamine 3000 (ThermoFisher Scientific: L300015). pGL3-Luc and Renilla constructs were used as controls for the transfection procedure. Cells were scraped and collected using the Promega Dual Luciferase Assay Kit (Promega: E1910) provided lysis buffer. Luciferase activity was measured using a luminometer with two injectors: the first containing the kit provided Luciferase substrate and the second containing the Stop-Glo substrate. Data was analyzed to account for background Renilla fluorescence activity. Data values were then normalized and compared to control.

2.3.7 Iron Response Element-Cyano Fluorescent Protein (IRE-CFP): Visual analysis of intracellular iron content

Iron Response Element - Cyan Fluorescent Protein (IRE-CFP) plasmid was kindly provided by Dr. James R. Connor at Penn State Hershey Medical Centre [78]. Transfection of IRE- CFP into L6 skeletal muscle cells was completed according to manufacturer's protocol (Lipofectamine 3000® [Invitrogen #L3000015]), directly onto glass cover slips (Fisher Scientific #12-546) in a 12 well plate (Falcon via VWR # 353043). After 2 days of incubation in a CO_2 incubator at 37°C, cells were starved in 0.5% FBS DMEM and treated with 250μm of $FeCl_3$ for 24h. Cells were washed 3X with PBS^{++} (supplemented with 1% Ca^{2+} and 1% Mg^{2+}), and fixed with 4% paraformaldehyde (PFA) (Sigma-Aldrich #HT501128) for 20 minutes. Cells were incubated in

1% glycine (Bioshop #GLN001.5) dissolved in PBS^{++} for 10 minutes and mounted onto glass slides with mounting medium (mixture of Prolong Anti Fade [Invitrogen #P36930] to Mounting Medium for Fluorescence with DAPI [Vectasheild/Vector Labs #H-1200] in a 3 to 1 ratio). Slides were observed with an LSM 700 confocal microscope with DAPI and FITC channels. Pixel intensity per cell was quantified using ImageJ software. IMARIS software was used to create representative 3D images.

2.3.8 DCF-DA: Characterization of IO induced intracellular ROS production

A plate-based assay used to confirm IO induced ROS production. DCF-DA is a fluorgenic dye that is oxidized by ROS to produce DCF which is the fluorescent component of the dye. The fluorescence is detected as an area scan at an excitation/emission spectra of 495/529nm. Data values normalized and compared to control.

2.3.9 Statistical analysis

Unpaired Student's T-test was conducted for determining statistical significance using GraphPad Prism. Data was presented as mean ± SEM. Statistical significance between treatment groups were calculated using the unpaired Student t test when comparing 2 groups. P value < 0.05 was considered statistically significant.

2.4 Results
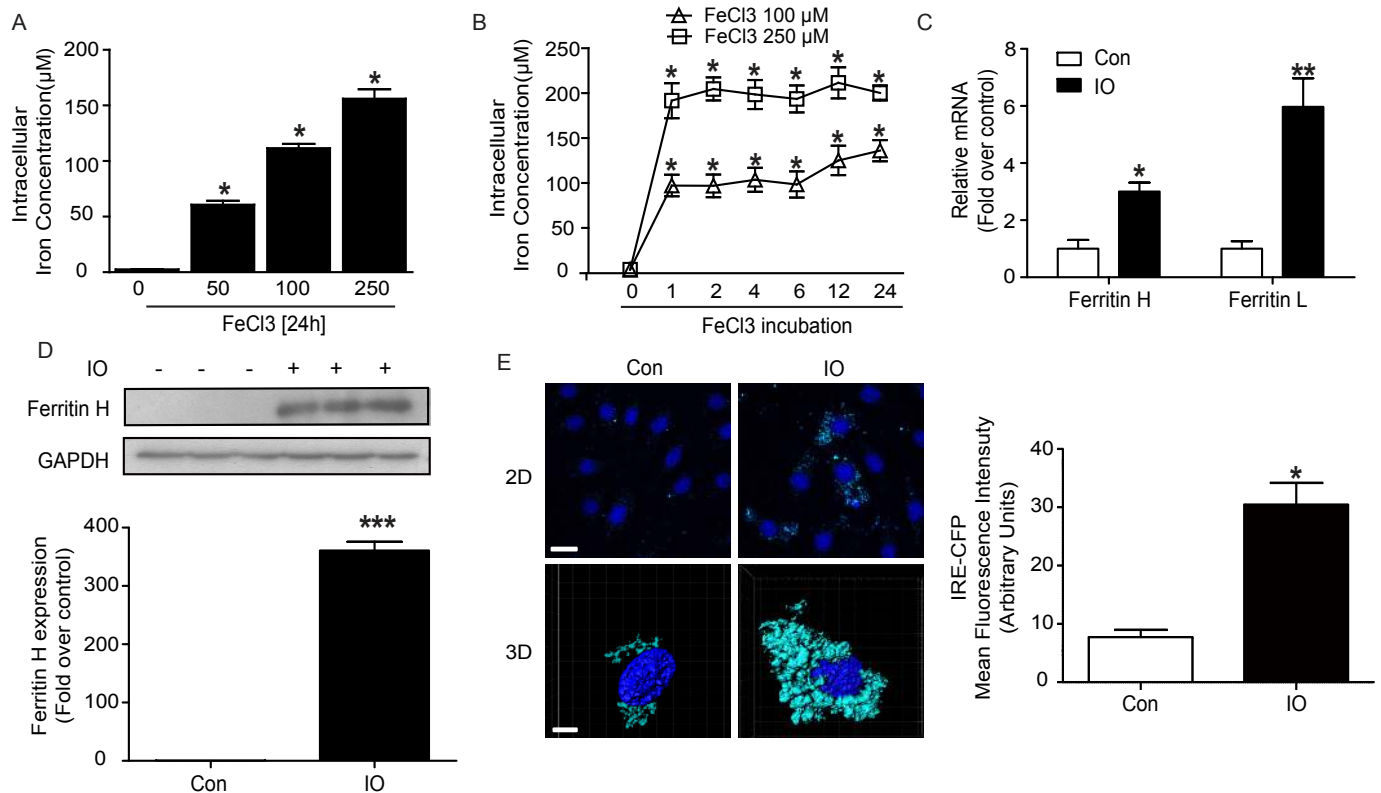
Figure 2.1 – Validation of cellular model for intracellular iron overload

(A) Dose response showing intracellular iron content in L6 skeletal muscle cells, detected using Ferrozine assay. Cells were treated with FeCl$_3$ at 50, 100 and 250 µM for 24h (n=3). (B) Time course using ferrozine assay in cells treated with 100µM and 250 µM FeCl$_3$ for 1,2,4,6,12 and 24h (n=3) (C) Relative mRNA levels of ferritin heavy and light chains determined by qPCR in untreated (Con) or cells treated with FeCl$_3$ - 250µM, 24h, (n=3) (IO). (D) Western Blot analysis of ferritin (~25 kDa) expression ± IO (n=3). (E) Cells expressing an IRE-driven CFP reporter were treated ± IO (n=3) and then 2-dimensional (2D) representative images were taken (scale bar: 2µM) or 3D representative images created from serial optical sections using IMARIS software (scale bar: 10µM). For quantitation, mean fluorescent intensity per cell was calculated. All graphs show mean ± SEM and * = P<0.05, ** = P<0.01, *** = P<0.001 versus Con.

2.4.1 Characterizing IO in L6 skeletal muscle cells

Figure 1 exhibits a series of experiments designed to optimize the IO dose and time course required for establishing the IO model. Fig.1(A) displays dose-response data obtained from a ferrozin colorimetric assay using 50μM, 100μM and 250μM of $FeCl_3$ for 24 hours. Data shows steady and proportionate increase in intracellular iron with 250μM displaying the greatest amount of intracellular iron. Fig.1(B) displays data obtained from a time course based Ferrozin colorimetric assay (0,1,2,4,6,12 and 24h) using 100μM and 250μM of $FeCl_3$. Results show that at 250μM, total intracellular iron content remained relatively constant along the time course, hovering around 200μM. There was a slight increase observed at the 12h and 24h timepoint upon exposure to 100μM of $FeCl_3$. Ferritin levels were examined at both the mRNA level and protein level with results displayed in figure 1, panels C and D respectively. Relative mRNA levels of both Ferritin Heavy chain (H) and Ferritin Light chain (L) exhibited a significant increase relative to untreated samples. Ferritin H showed a highly significant increase in protein expression under IO treatment, fig.1(D), relative to control cells. Fig.1(E) exhibits images obtained via confocal microscopy displaying the effects of treating Iron Response Element-CyanoFluorescent Protein (IRE-CFP) transfected L6 cells with IO. The images and accompanying quantitation display a significant increase in mean fluorescence intensity relative to control.

37
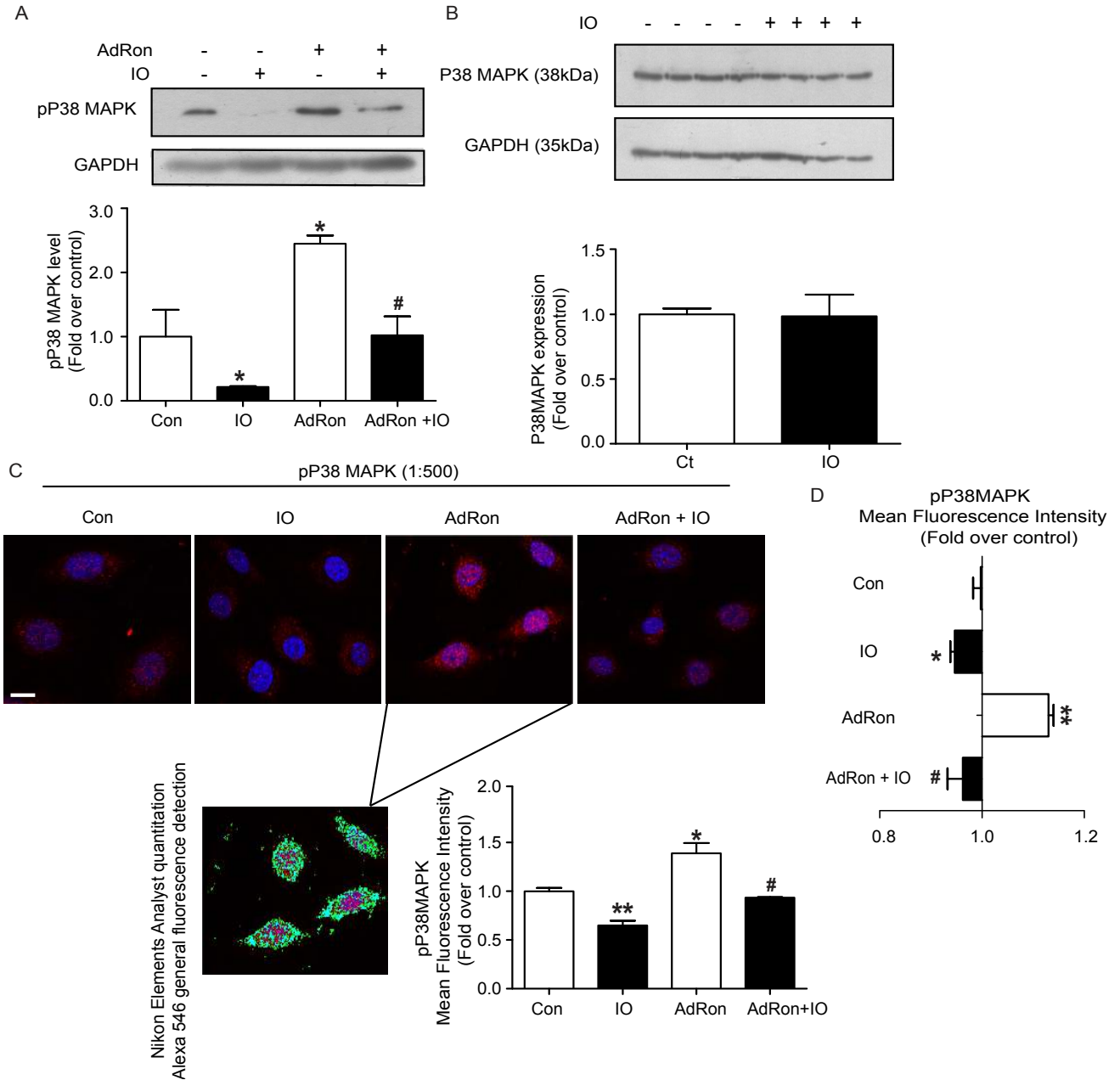
Figure 2.2 - Effects of IO on Adiponectin Signaling: P38 MAPK

(A-B) Western Blot data detailing the effects of IO (FeCl$_3$-250μM, 24h) and AdRon (35μM, 30min) treatment on phosphorylation of P38 MAPK and total P38 MAPK expression (~38 kDa) (n=4) (C) Immunofluorescence data from Nikon Confocal displaying effects of IO (FeCl$_3$-250 μM, 24h) and AdRon (35μM, 30min) treatment on phosphorylation of P38 MAPK (n=3) (Scale bar: 10 μM). For quantitation, mean fluorescent intensity for all cells in field of view was calculated via Nikon Elements Analyst software. (D) Immunofluorescence data

obtained from ThermoFisher Scientific's CX7 instrument. Data displays the effects of IO (FeCl$_3$-250µM, 24h) and AdRon (35µM, 30min) treatment on phosphorylation of P38 MAPK (n=4). All graphs show mean ± SEM and * = P<0.05, ** = P<0.01 versus Con, # = P<0.05 versus AdRon.

2.4.2 Adiponectin resistance in L6 skeletal muscle cells

Figure 2 displays the effects of IO (FeCl$_3$ 250µM, 24h) on adiponectin signaling via readout of P38 MAPK. Panel A and B displays the effects of IO treatment on phosphorylation of P38 MAPK and total P38 MAPK expression respectively. IO treatment resulted in a dramatic decrease in phosphorylation of P38 MAPK relative to control, while treatment with AdipoRon, an adiponectin agonist, displayed a significant increase in phosphorylation of P38 MAPK relative to control. Co-treatment of IO and AdipoRon resulted in a relatively higher degree of phosphorylation of P38 MAPK relative to IO, but lower than AdipoRon treatment alone. Panel B shows no change in total P38 MAPK protein expression post-IO treatment. The same phenomenon was observed when an Immunofluorescence (IF) assay was conducted with the same conditions (Panel C). There was an observed decrease in fluorescence under IO treatment relative to control, while AdipoRon treatment resulted in a significant increase in fluorescence relative to control. Co-treatment of IO and AdipoRon displayed a reduced intensity in fluorescence relative to AdipoRon alone and increased fluorescence relative to IO. Panel D exhibits the high throughput data obtained from the ThermoFisher CX7 system, showing an identical trend observed in Panel C with AdipoRon treatment resulting in increased fluorescence and IO treatment resulting in decreased fluorescence relative to control.
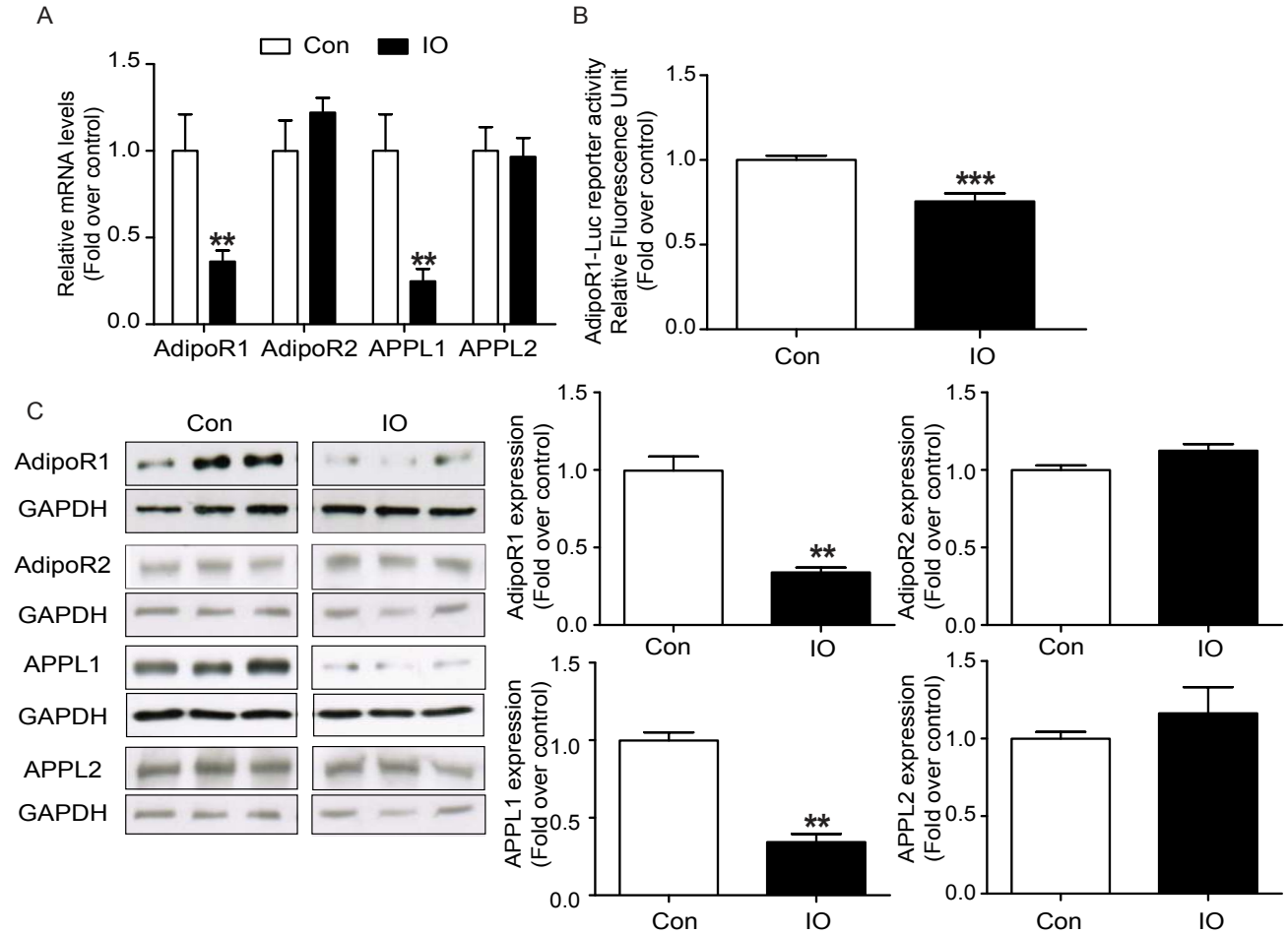
Figure 2.3 - Effects of IO on adiponectin receptors (AdipoR1/2) and associated proteins (APPL1/2)

(A) qPCR relative mRNA values of primary adiponectin receptors (AdipoR1/2) and adaptor proteins APPL1/2 post IO treatment (FeCl$_3$-250µM, 24h). Values were normalized to 18S housekeeping gene (n=4). (B) Dual Luciferase Reporter assay data using L6 cells transfected with AdipoR1_Luc reporter construct post IO treatment (FeCl$_3$-250µM, 24h) (n=4) (C) Western Blot data detailing the effects of IO treatment (FeCl$_3$-250µM, 24h) on protein expression levels of AdipoR1/2 (~50kDa) and APPL1/2 (~82kDa) (n=4). All graphs show mean ± SEM and * = P<0.05, ** = P<0.01 versus Con.

41

2.4.3 Adiponectin receptor expression and associated proteins

Adiponectin receptor levels were monitored at the mRNA level via qPCR. Fig.3(A) shows that

upon IO treatment, relative mRNA levels of AdipoR1 and APPL1 were significantly decreased

compared to control while mRNA levels of AdipoR2 and APPL2 showed no change. This trend

was also observed at the protein level via Western Blot (WB) in Fig.3(C). To determine

transcriptional activation of the AdipoR1 promoter, a Dual Luciferase Reporter Assay was

performed (Panel B) which showed that upon IO treatment, a significant decrease in

luminescence was detected relative to control conditions.
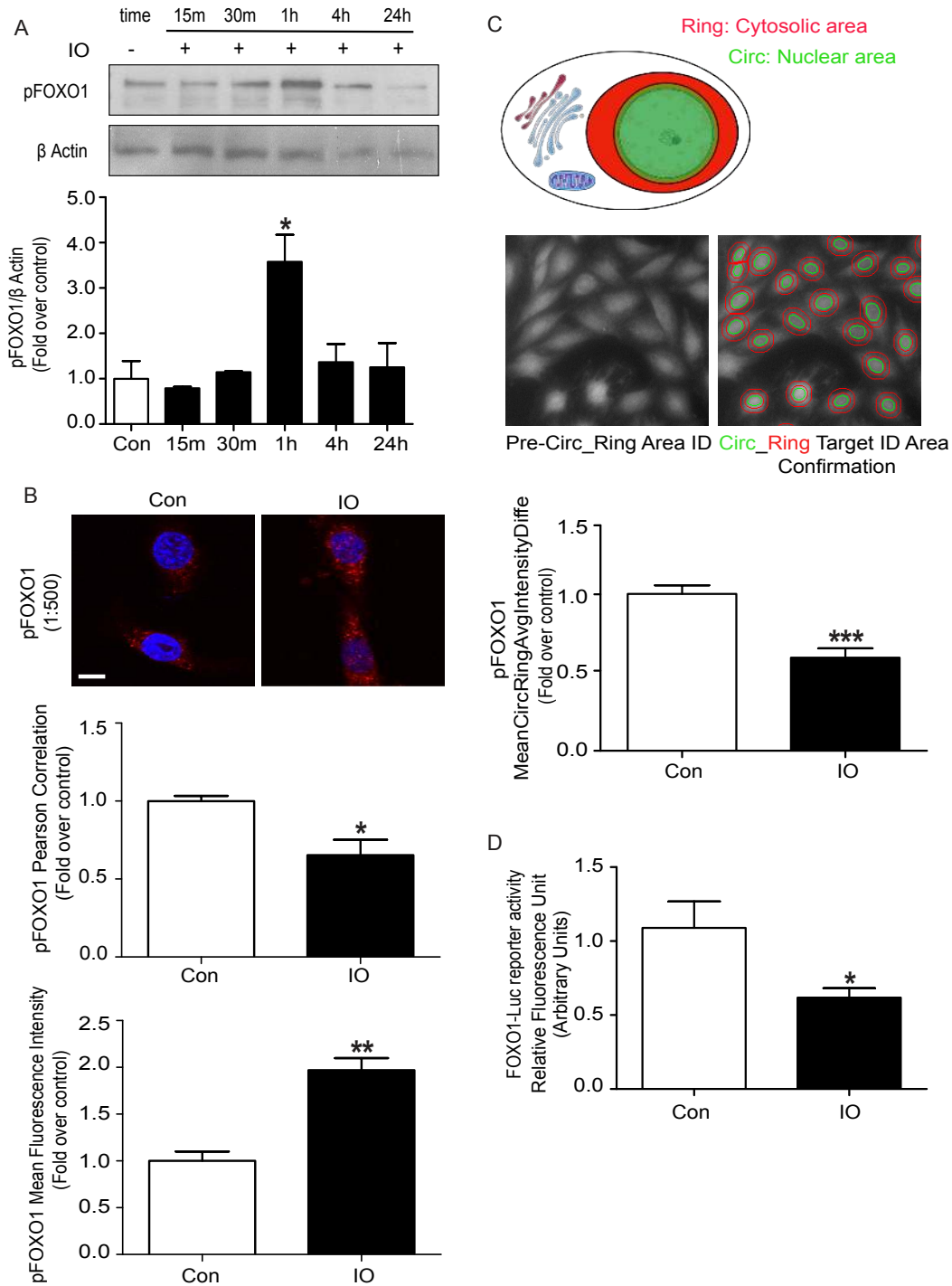
Figure 2.4: Regulation of FOXO1 by IO

(A) Western Blot results demonstrate the effects of IO (FeCl$_3$ - 250 μM) on phosphorylation of the transcription factor FOXO1 (~80kDa) at 15min, 30min, 1h, 4h and 24h (n=4). (B) ImmunoFluorescence of pFOXO1 post IO treatment (FeCl$_3$-250μM, 1h) from Nikon Confocal microscope (n=3). Mean Fluorescence Intensities were detected and

recorded for all cells in field of view via Nikon Elements Analyst software. ImageJ plugin JACop was used to obtain Person Correlation Coefficient values of nuclear overlap of pFOXO1 (Scale bar: 10 µM) (C) CX7 quantification data of Immunofluorescence based molecular translocation assay for pFOXO1 (Primary antibody: 1:50) post IO treatment (FeCl$_3$-250µM, 1h) (n=4). Parameters measured was mean CircRingAvgIntensityDifference which correspond to the average intensity difference of fluorescence emitted by the secondary antibody (Alexa546 - 1:200) between the designated Circ (nuclear area - green in schematic) and Ring (cytosolic area - red in schematic). A "negative" or decrease in value corresponds to greater fluorescence detected from the cytosol. (D) Dual Luciferase Reporter assay data using L6 cells transfected with FOXO_Luc reporter construct post IO treatment (FeCl$_3$-250µM, 24h) (n=3). All graphs show mean ± SEM and * = P<0.05, ** = P<0.01, *** = P<0.001 versus Con.

2.4.4 Regulation of FOXO by Iron

Post translational modification (PTM) of FOXO1 due to IO treatment was examined initially via WB. As shown in Fig.4(A), upon a time course assessment of the phosphorylation status of FOXO1, the results displayed a significant increase in phosphorylation of FOXO1 at the 1h time point. An IF based approach was used to examine potential changes in localization of FOXO1 due to its PTM. Fig.4(B) shows an increase in fluorescence of pFOXO1 under IO treatment. A Pearson's Correlation analysis was performed to determine the degree of colocalization of pFOXO1 with regards to cytosol vs nucleus. The analysis revealed a decrease in value of Pearson's Correlation upon IO treatment with regards to pFOXO1. ThermoFisher Scientific's CX7 instrument was used to further assess pFOXO1 localization. Fig.4(C) shows a significant decrease in the mean CircRingAvgIntensity difference of pFOXO1 under IO conditions. FOXO1 transcriptional activity (Fig.4(D)) was determined using a Dual Luciferase Reporter Assay whereby upon IO treatment, a significant decrease in fluorescence was detected relative to control.
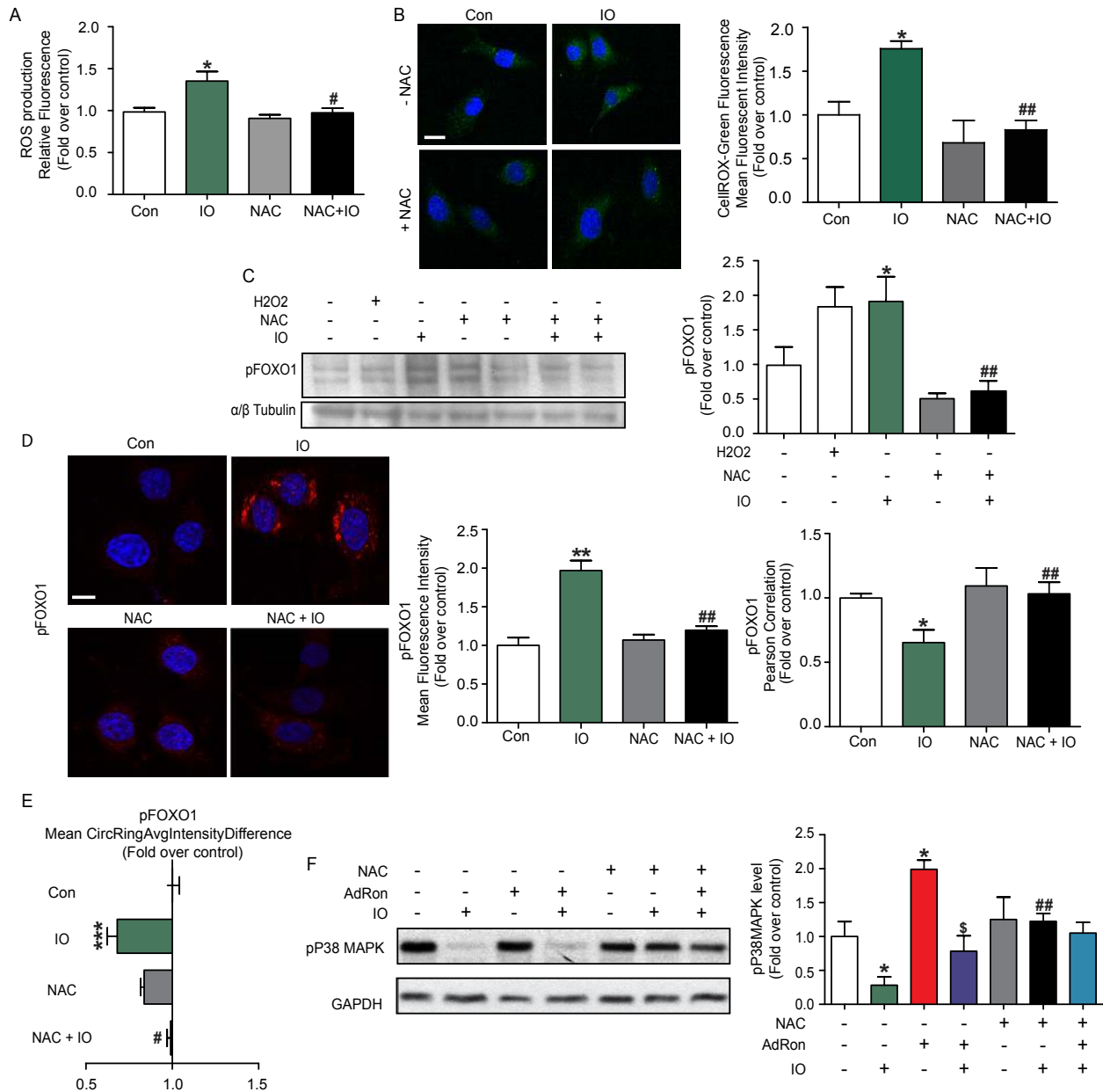
Figure 2.5: Mechanistic role of Oxidative Stress in FOXO regulation and adiponectin signaling by iron

(A) DCF-DA assay used to determine the total amount of ROS produced post IO treatment of L6 cells (FeCl₃-250 µM, 1h). NAC (N-Acetyl Cysteine-500nM, 30 minutes) used as a ROS inhibitor prior to iron treatment (n=3). (B) CellROX Green (2.5 µM, 30minutes) fluorescence-based assay displaying the effects of IO treatment (FeCl₃-250 µM, 1h) on the production of ROS. NAC (N-Acetyl Cysteine-500nM, 30 minutes) used as a ROS inhibitor prior to iron treatment. Mean Fluorescence Intensity was detected and

analyzed for all cells in field of view using the Nikon Elements Analyst software (Scale bar: 10 μM) (n=4). (C) Western Blot data displaying the effect of IO (FeCl$_3$-250 μM, 1h) induced ROS production on the phosphorylation status of FOXO1 (~80 kDa). Positive control H$_2$O$_2$ used at 200 μM for 30min. NAC (N-Acetyl Cysteine-500nM, 30 minutes) used as a ROS inhibitor prior to iron treatment (n=9). (D) ImmunoFluorescence of pFOXO1 post IO treatment (FeCl3-250 μM, 1h). NAC (N-Acetyl Cysteine-500nM, 30 minutes) used as a ROS inhibitor prior to iron treatment. Mean Fluorescence Intensity was detected and analyzed for all cells in field of view using the Nikon Elements Analyst software. ImageJ plugin JACop was used to obtain Person Correlation Coefficient values of nuclear overlap of pFOXO1 (Scale bar: 10 μM) (n=3) (E) CX7 quantification data of ImmunoFluorescence based molecular translocation assay for pFOXO1 post-IO treatment (FeCl$_3$-250μM, 1h). NAC (N-Acetyl Cysteine-500nM, 30 minutes) used as a ROS inhibitor prior to iron treatment. Parameters measured was mean CircRingAvgIntensityDifference which correspond to the average intensity difference of fluorescence emitted by the secondary antibody (Alexa546 - 1:200) between the designated Circ and Ring area. A "negative" or decrease in value corresponds to greater fluorescence detected from the cytosol (n=4) (F) Western Blot data displaying the effects of IO induced (FeCl$_3$-250 μM, 24h) ROS production on the phosphorylation status of P38MAPK. P38MAPK activation was induced with adiponectin receptor agonist, AdRon, at 35 μM for 30min. NAC (N-Acetyl Cysteine-500nM, 30 minutes) used as a ROS inhibitor prior to iron treatment (n=9). All graphs show mean ± SEM and * = P<0.05, ** = P<0.01 versus control, #=P<0.05, ##=P<0.001 versus IO and \$=P<0.05 relative to AdRon.

47

2.4.5 Mechanistic Role of Oxidative stress in FOXO regulation

IO induced oxidative stress was assessed with two separate experiments. The first, a DCF-DA plate based assay, (Fig.5(A)), revealed that upon IO treatment, a significant increase in relative fluorescence was observed relative to control. The treatment of NAC in conjunction with IO reversed this effect. Fig.5(B) showed the results obtained through the use of confocal microscopy to determine the degree of IO induced oxidative stress using CellROX Green. The same experimental conditions were used and under IO, there was a significantly greater fluorescence detected compared to control. This effect was, again, reversed upon co-treatment of the L6 cells with both NAC and iron. To determine the effect of IO induced ROS on the PTM status of FOXO1, a WB and IF approach were used (Fig.5(C) and (D) respectively). Fig.5(C) shows that upon IO treatment, there is a significant increase in phosphorylation of FOXO1 relative to control while administration of NAC with IO reverses this effect. With regards to Fig.5(D), treatment of L6 cells with IO exhibited a significant increase in fluorescence of pFOXO1. Treatment of NAC in conjunction with iron significantly decreased the mean fluorescence intensity compared to iron alone. In terms of localization, the Pearson's Correlation was analyzed and it was determined that upon IO treatment, there was a reduction in Pearsons Correlation of pFOXO1. This effect was reversed upon co-treatment with both NAC and iron. Upon examination of the data generated by ThermoFisher Scientific's CX7 (Fig.5(E)) with regards to pFOXO1 under IO treatment, there was a significant decrease in the CircRingAvgIntensity difference relative control. This effect was reversed upon co-treatment of NAC with iron. The effects of IO induced ROS production on adiponectin signaling was examined via pP38 MAPK. Fig.5(F) shows that upon treatment of iron, there was a significant decrease in the phosphorylation of P38 MAPK relative to control, while the administration of AdipoRon significantly increased the degree of phosphorylation of P38 MAPK relative to control. Co-treatment of AdipoRon and iron resulted in a greater degree of phosphorylation of P38 MAPK relative to IO, but lower than that of AdipoRon

48

alone. Treatment of NAC in the presence of iron reversed the effect of IO alone with an observed

greater degree of phosphorylation.

2.5 Discussion

Numerous groups have focused their efforts on elucidating the precise mechanisms that govern the basis of which metabolic diseases occur. The complexity of the matter presents a unique set of challenges which explains why understanding metabolic disorders, such as T2D, remains a difficult, yet fertile ground for research. With regards to T2D, several studies were conducted and a consistent trend has been observed with regards to iron's role. By monitoring serum ferritin levels in prospective studies, at least 5 studies that examined a wide range of otherwise healthy men and women of different backgrounds, aged 40 - 60, showed that those with higher iron stores were on average 2.4 times more likely to develop T2D when compared to those with lower iron stores [22,24,92,93,94,95]. Further observational studies, in addition to clinical trials, were conducted to assess the effects of iron depletion on insulin sensitivity and glucose tolerance. The results, summarized from one observational study and 3 clinical trials, found that regardless of iron depletion method (increased blood donations or phlebotomy therapy) individuals exhibited lower ferritin levels, improved insulin sensitivity and an overall reduction in insulin resistance [69,70,71,72]. There are several theories behind how iron exerts this effect. One theory, shown in a Hereditary Hemochromatosis mouse model, is that increased iron stores in skeletal muscle was found to cause a shift in fuel utilization from glucose to free fatty acids [73]. This shift was shown to increase hepatic glucose production and release, thereby contributing to the hyperglycaemic condition pertaining to T2D [73]. Another contributing factor is the susceptibility of pancreatic beta cells to become overloaded with iron due to presence of promiscuous divalent metal ion channels which directly contribute to the decrease in insulin production and secretion [24,88].

However, the theory with the most traction with regards to iron's effect, is it's ability to induce a state of increased oxidative stress. This is due its pro-oxidant properties, which drives reactions, such as the electron transport chain (ETC) in the mitochondria, to generate high amounts of ROS. In the case of pancreatic beta cells, their heavy reliance on the mitochondria

50

makes them highly susceptible to damage due to oxidative stress and thus impairs their ability to produce insulin [22,23,87].

Considering adiponectin's insulin sensitizing properties, as well as the decrease observed in serum adiponectin levels in the presence of high levels of ferritin, it was of vital importance to elucidate the mechanism by which iron induces this effect. Adiponectin action is facilitated by binding of the adipokine to one of it's two primary receptors Adiponectin Receptors: AdipoR1 and AdipoR2 [42,82]. It is well established that both receptors are ubiquitously expressed in all tissues, however, some studies report a greater abundance of AdipoR1 in skeletal muscle while AdipoR2 is more commonly found in the liver [40]. Upon binding of adiponectin to its receptor, the adaptor protein APPL1 proceeds to activate a series of kinases that in turn mediate adiponectin's effect through a variety of signaling pathways, most notably AMPK, P38 MAPK and PPAR-α [44,82]. We have successfully demonstrated that upon inducing a state of IO, a decrease in the mRNA and protein expression of AdipoR1 and APPL1 was observed. The lack of change seen in AdipoR2 and APPL2 levels could be attributed to the relative abundance of these proteins in liver cells, as previously described. AdipoR1 promoter activity was examined via a luciferase reporter assay and it was determined that upon IO treatment, a clear and significant decrease in the luminescence was detected. This suggests that the AdipoR1 promoter activity decreases as a result of IO treatment, which is consistent with the observed decrease in AdipoR1 mRNA levels and protein levels observed previously.

As mentioned previously, one of the effector proteins that mediates adiponectin action is P38 MAPK. Upon binding of adiponectin to AdipoR1, APPL1 activates two different protein kinases, TAK1 and MKK3, which then proceed to phosphorylate and activate P38 MAPK [52]. Activation of P38 MAPK has been linked to direct stimulation of PPAR-α transcriptional activity, which is essential for fatty acid oxidation, reduction in triglycerides and improved insulin sensitivity in both liver and skeletal muscle [48,96]. P38 MAPK activation has also been linked to increased plasma translocation of glucose transporter GLUT4 prompting increased glucose uptake [50,53,96].

51

In order to assess whether IO results in adiponectin resistance, P38 MAPK protein expression levels were examined via Western Blot (WB) and immunofluorescence means. Activation of P38 MAPK was mediated through AdipoRon, a synthetic small molecule that acts as a potent AdipoR agonist. We have shown that AdipoRon greatly increased phosphorylation of P38 MAPK while IO treatment resulted in impaired phosphorylation of P38 MAPK relative to control. Co-treatment of both AdipoRon and iron resulted in a decrease in phosphorylation of P38 MAPK relative to AdipoRon alone thus suggesting adiponectin signaling impairment. This data suggests that the treatment of L6 cells with IO induces a state of adiponectin resistance.

Since AdipoR1 was impacted at the transcriptional level, as evident by the decrease in promoter activity, it was only logical to explore the primary transcription factor responsible for a potential mechanism behind how iron enforces its effect. Several studies have highlighted the importance of FOXO1 in the field of metabolism. Its role in insulin signaling via PI3K activation has long been established and numerous papers have shown its proclivity to act as a transcription factor responsible for transcribing adiponectin and its receptors [64]. Therefore, the next step in elucidating a possible mechanism behind IO induced adiponectin resistance was to examine iron's effects on FOXO1. It is widely understood that transcription factor activity is largely dictated by its post translational modifications (PTM). Once FOXO1 is phosphorylated, the TF translocates to the cytoplasm effectively reducing its function as a TF [55,89]. Upon examining the phosphorylation status of FOXO1 from a time course approach, it was evident that maximal phosphorylation of FOXO1 occurred at 1h post-IO treatment. Through IF means, we have shown that upon IO treatment, there was an observed increase in cytoplasmic localized pFOXO1 relative to control as indicated by the increased cytoplasmic fluorescence observed. In terms of total FOXO1, we see a high degree of nuclear fluorescence being emitted under control conditions that is diminished upon IO treatment. These observations confirm the notion that IO results in increased phosphorylation of FOXO1 resulting in cytosolic localization.

To determine whether the theory of iron induced oxidative stress applies to the case of IO induced adiponectin resistance, we have successfully demonstrated that upon use of synthetic ROS inhibitor, N-acetyl-L-Cysteine (NAC), the observed effects of iron on FOXO1 phosphorylation and adiponectin signaling via P38 MAPK were reversed. NAC is a synthetic precursor to naturally occurring antioxidant defence systems. It exerts its function by either activating the redox potential of thiols or by increasing glutathione levels which when combined acts as a free-radical scavenging system [74]. The phosphorylation status of FOXO1 was investigated via WB and immunofluorescence in order to determine relative localization. As expected, Phosphorylation of FOXO1 increased with IO treatment and this effect was reversed upon treatment of NAC. The same trend was observed, figure 5(D), via immunofluorescence where IO treatment increased cytosolic fluorescence of pFOXO1 relative to control and that NAC reversed this effect resulting in decreased cytosolic localization of pFOXO1. Collectively, this data suggests that IO induced oxidative stress results in an increase in the phosphorylation of FOXO1, localizing it to the cytosol and possibly reducing its capacity to act as a transcription factor.

The same approach was used to determine whether IO induced oxidative stress could be attributed to the decrease in adiponectin signaling observed. Phosphorylation of P38 MAPK was examined under IO conditions which resulted in the expected decrease in activation of P38 MAPK. Treatment with AdipoRon resulted in increased phosphorylation of P38 MAPK relative to control, suggesting P38 MAPK activation. Co-treatment of AdipoRon and IO resulted in a lowered the degree of phosphorylation of P38 MAPK suggesting impaired AdipoRon activation of P38 MAPK. Upon treatment of NAC in the presence of IO, the effects of IO were reversed. This suggests that the ROS produced by IO is responsible for the decreased activation of P38 MAPK which results in impaired adiponectin signaling.

It is clear that iron's effects are multivariate and that there is no parsimonious explanation that can be attributed to its role in T2D. The IO-ROS-FOXO1-AdipoR1 axis is only one possible explanation to this phenomena. This axis still requires further study to uncover the finer details

such as irons effect on TAK1 and MKK3 which would explain how the reduction in P38MAPK phosphorylation occurs. Oxidative stress has been shown to influence FOXO activity which is why this family of transcription factors is instrumental in facilitating a response. Examples include increased phosphorylation of FOXO3 and FOXO4 by MST1 and JNK respectively [57]. Phosphorylation of FOXO3 by MST1 has been shown to increase transcription of the antioxidant defence protein MnSOD [57]. An important point to note is that cell type and FOXO isoform can have seemingly conflicting functions. Under IO conditions in adipocytes, FOXO1 is reportedly deacetlyated, leading to increased binding to PPAR-RE resulting in decreased AdipoR1 transcription [63]. It is therefore within the realm of possibility that IO induced oxidative stress can result in increased kinase activity in skeletal muscle. This mechanism would require further investigation. Iron's effects, as previously described, have far reaches and can severely impair mitochondrial and ER function. Another avenue worth exploring is what role, if any, mitochondrial dysfunction has in the development of iron induced adiponectin resistance. The outer-mitochondrial membrane protein MitoNEET, for example, regulates the amount of iron entering the mitochondria and in cases of IO, MitoNEET levels have been observed to be decreased resulting in mitochondrial iron loading and mitochondrial dysfunction [75]. Studies have shown that mitochondrial dysfunction results in the accumulation of triacylglycerides which in turn activate a series of protein kinases, such as protein kinase C, that in turn impair insulin signaling [76]. Could there be a link between mitochondrial dysfunction and adiponectin resistance as well? IO induced ER stress has been reported to result in decreased expression of ERp46, a protein that has been documented to interact with AdipoRs and is responsible for chaperone folding and retrograde/anterograde shuttling of the receptor to the PM [77]. This could be another potential mechanism as to why there is an observed decrease in AdipoR1/2.

In conclusion, one mechanism has been thus far uncovered with regards to IO induced adiponectin resistance in L6 skeletal muscle cells. IO was found to induce the production of ROS which in turn played an effector role in increased phosphorylation and cytosolic localization of

54

FOXO1. This change in localization of FOXO1 resulted in decreased adiponectin receptor promoter activity and protein expression of AdipoR1. The IO induced oxidative stress also resulted in impaired adiponectin signalling, as indicated by the decrease in phosphorylation and activation of the adiponectin signalling molecule, P38 MAPK. Treatment of NAC, a non-specific ROS inhibitor, reversed IO's effects on both FOXO1 phosphorylation, localization and P38 MAPK inactivation further confirming that adiponectin resistance can be attributed to IO induced ROS production.

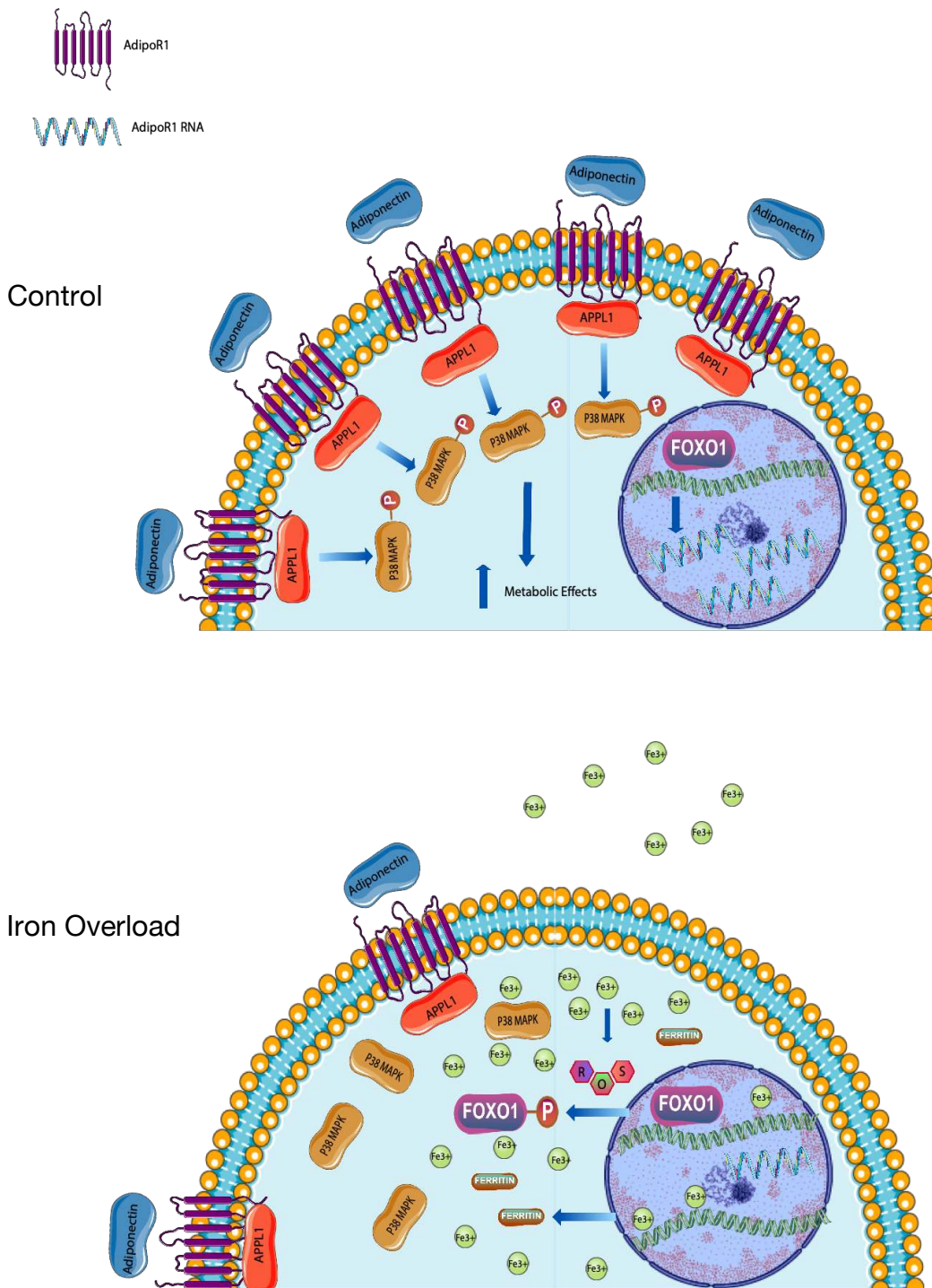**Figure 2.6: Summary schematic detailing IO induced adiponectin resistance via an oxidative stress mechanism whereby IO ROS produced leads to increased FOXO1 phosphorylation and cytosolic translocation propogates decreased transcription of AdipoR1 and reduced APPL1 activation resulting in impaired adiponectin signaling as evident by decreased phosphorylation of P38 MAPK.**

Chapter 3: Future Directions

With regards to future directions, there are many avenues worth exploring that could potentially propagate the impact of this work. Several of these are briefly mentioned in the discussion section of the previous chapter but will be discussed in more detail below.

Firstly, with the current proposed mechanism of IO induced adiponectin resistance, additional details can be further elucidated. Most important of which involve FOXO1 regulation. The current mechanism suggests phosphorylation as the PTM responsible for FOXO1 cytosolic localization. However, our data (figure 4.1B) indicates that IO additionally increases FOXO1 acetylation, which has also been attributed to increased cytosolic localization [90]. Acetylation and phosphorylation could present a dual mechanistic explanation regarding iron's effect. The players that facilitate these PTMs, acetylases such as CBP/p300 and kinases such as Akt, MST1, CDK1/2 and AMPK have all been shown to react to states of oxidative stress resulting in varied cell-specific FOXO1 effects [90]. It is therefore crucial to understand which kinases or acetylases are responsible for the observed IO induced FOXO1 PTMs to fully complete the picture regarding this proposed mechanism.

Secondly, mitochondrial dysfunction has been a prominent mechanistic candidate regarding the etiology of T2D. An observed decrease in mitochondrial content, in addition to reduced beta oxidation activity results in the increase of diaceyl glycerol and fatty acids [97]. This facilitates the activation of isoforms of PKC, as previously suggested, leading to the phosphorylation of IRS-1 on Ser^{307} resulting in decreased PI3K and Akt activation and thus impairing glucose uptake [97]. A similar mechanism regarding mitochondrial dysfunction could also be prevalent in the case of IO induced adiponectin resistance. Since the mitochondria is one of the main sites of ROS production due to the ETC [87], and with iron being a cofactor in this reaction, it is plausible that this mechanism could perhaps play a role in development of adiponectin resistance. The leakage of electrons from complexes I and III result in the production of superoxide, which ferric iron can react with producing highly reactive hydroxyl radicals [87]. With

that said, it is important to determine if IO results in increased mitochondrial ROS production and whether this plays a role in the development of adiponectin resistance. This can be investigated with the use of mitochondrial complex I inhibitors such as rotenone [98].

MitoNEET, an outer mitochondrial membrane protein responsible for regulating iron entry, has been shown to be impaired under IO conditions, resulting in the overloading of the mitochondria with iron [75]. Preliminary work has been conducted with regards to investigating this mechanism via the use of mitoferrofluor (MFF). MFF is a mitochondrial specific probe that is designed to be quenched in the presence of iron [97]. Figure 4.2(C-D) display a clear decrease in fluorescence detected from the probe under IO conditions in addition to exhibiting a high degree of co-localization with the mitochondrial marker TOM20. Furthermore, there is also an observed decrease in TOM20 signal that could indicate a compromised mitochondrial health and decreased biogenesis, all features of mitochondrial dysfunction which may play a role in adiponectin resistance. These findings could provide further insight into mechanisms that potentially explain how/where IO induced ROS is generated in parallel to the role oxidative stress plays in adiponectin resistance.

An important avenue to note and further explore are the other possible routes IO can induce oxidative stress. While it is well established that iron can increase the production of reactive hydroxyl radicals through the Haber-Weis/Fenton reaction, there are other possible candidates at play [21,35]. Studies have reported, as previously described, impaired antioxidant defence mechanisms such as reduced SOD proteins under IO conditions [21]. This begs the question of whether IO indeed results in elevated ROS, or was the observed increase in oxidative stress due to impaired antioxidant defences rather than ROS emission? SOD inhibitors, such as diethyldithiocarbamate, can be employed here to confirm the effects of IO and whether elevated oxidative stress is a result of a dual effect [99]. These findings could provide further insight into

mechanisms that potentially explain how/where IO induced ROS is generated in parallel to the role oxidative stress plays in adiponectin resistance.

Thirdly, in cases of adiponectin resistance observed in heart failure cases, adiponectin receptor phosphorylation has been suggested to potentially play a role via the internalization of the receptors and impairment of adiponectin signaling [47]. Phosphorylation of AdipoR1 in a post-myocardial infarction (post-MI) model was observed at Ser^7, Thr^{24} and Thr^{53} by the kinase GRK2 [47]. This mechanism could be worth exploring in a skeletal muscle model under IO since GRK2 has been showing to physically interact with AdipoR1. ERp46 is another protein responsible for the retro/anterograde transport of AdipoR1/2 to/from the endoplasmic reticulum [77]. The levels of ERp46 could potentially be altered under IO, which has been linked to ER stress, and could possibly provide another mechanistic rationale behind the decrease in observed AdipoR1 protein levels and impaired adiponectin signaling.

Finally, to cement the findings described in this work, the ultimate goal would be to replicate these findings in an *in vivo* model. The challenge with this objective, as in any *in vivo* model, is to account for iron's multifactorial effect that could potentially alter various systems already in place in addition to the broad role of TFs such as FOXO1 plays. This disturbs the delicate dynamic present which would make attributing IO induced adiponectin resistance to the proposed mechanism a great challenge.

Chapter 4: References and supplementary data
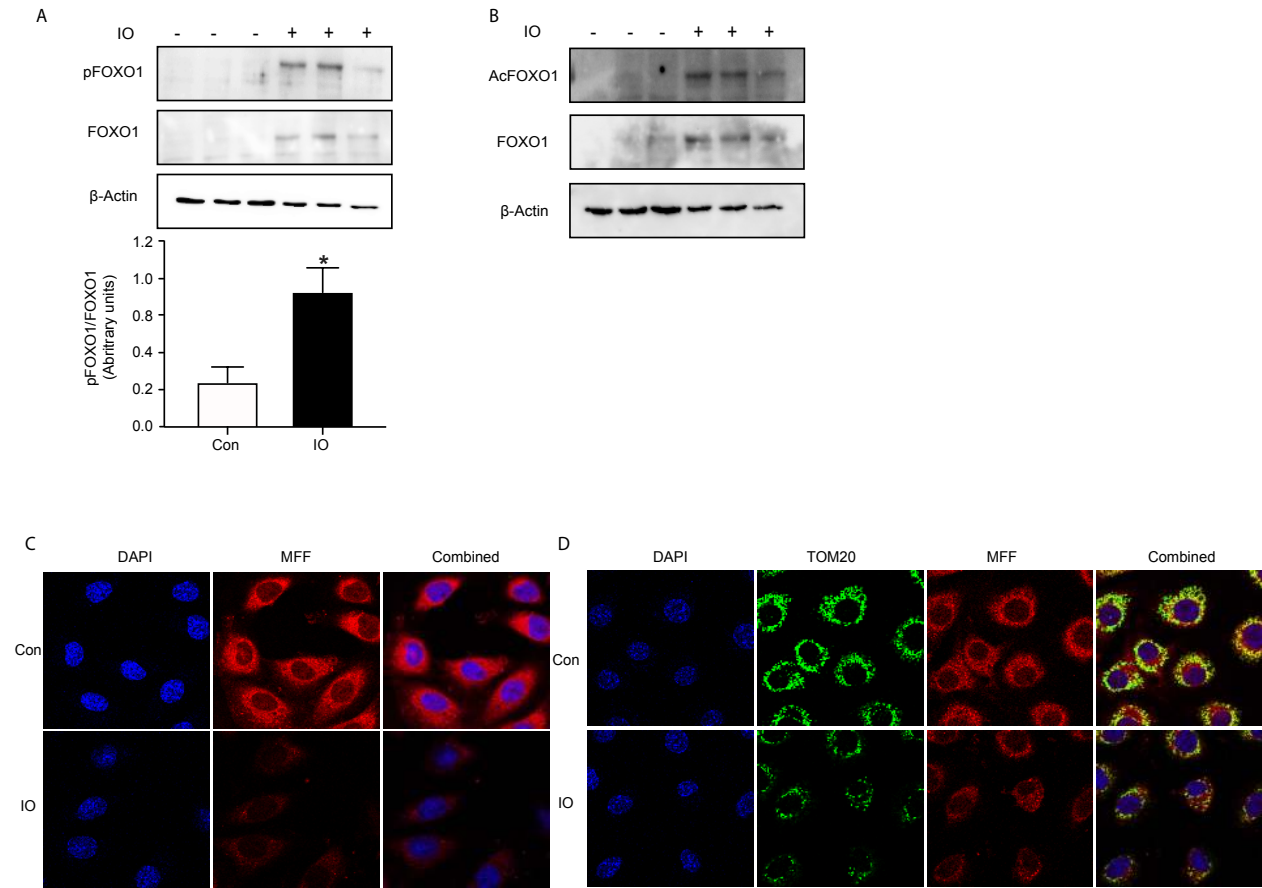
Figure 4.1: (A-B) WB exhibiting FOXO1 PTM (phosphorylation n=3 and acetylation n=2 respectively) versus total FOXO1 (~80 kDa) under IO conditions (FeCl$_3$ - 250 µM, 24h). (C-D) IF data using MitoFerrofluor (MFF, 1 µM), a mitochondrial specific iron probe that is quenched in the presence of iron. Conditions tested were FeCl$_3$ - 250 µM, 24h (n=3). Panel D (n=1) shows same conditions with the addition of TOM20 (1:200), a primary antibody that binds to the outer membrane of the mitochondria.

4.2 References

1. Noncommunicable diseases: Fact sheets, World Health Organization, 1 June 2018, https://www.who.int/news-room/fact-sheets/detail/noncommunicable-diseases

2. Cardiovascular diseases (CVDs): Fact sheets, World Health Organization, 17 May 2017, https://www.who.int/news-room/fact-sheets/detail/cardiovascular-diseases-(cvds)

3. Obesity and overweight: Fact sheets, World Health Organization, 16 February 2018, https://www.who.int/news-room/fact-sheets/detail/obesity-and-overweight

4. Eckel, R. H., Grundy, S. M., & Zimmet, P. Z. (2005). The metabolic syndrome. *The lancet*, *365*(9468), 1415-1428.

5. Grundy, S. M. (2004). Obesity, metabolic syndrome, and cardiovascular disease. *The Journal of Clinical Endocrinology & Metabolism*, *89*(6), 2595-2600.

6. Saklayen, M. G. (2018). The global epidemic of the metabolic syndrome. *Current hypertension reports*, *20*(2), 12.

7. Després, J. P., & Lemieux, I. (2006). Abdominal obesity and metabolic syndrome. *Nature*, *444*(7121), 881.

8. Alberti, K. G. M. M., Eckel, R. H., Grundy, S. M., Zimmet, P. Z., Cleeman, J. I., Donato, K. A., ... & Smith Jr, S. C. (2009). Harmonizing the metabolic syndrome: a joint interim statement of the international diabetes federation task force on epidemiology and prevention; national heart, lung, and blood institute; American heart association; world heart federation; international atherosclerosis society; and international association for the study of obesity. *Circulation*, *120*(16), 1640-1645.

9. Attie, A. D., & Scherer, P. E. (2009). Adipocyte metabolism and obesity. *Journal of lipid research*, *50*(Supplement), S395-S399.

10. Grundy, S. M. (2016). Metabolic syndrome update. *Trends in cardiovascular medicine*, *26*(4), 364-373.

11. Diabetes: Fact sheets, World Health Organization, 30 October 2018, https://www.who.int/news-room/fact-sheets/detail/diabetes

12. Federation, I. D. (2013). IDF diabetes atlas. *Brussels: International Diabetes Federation*.

13. Hameed, I., Masoodi, S. R., Mir, S. A., Nabi, M., Ghazanfar, K., & Ganai, B. A. (2015). Type 2 diabetes mellitus: from a metabolic disorder to an inflammatory condition. *World journal of diabetes*, *6*(4), 598.

14. Aggoun, Y. (2007). Obesity, metabolic syndrome, and cardiovascular disease. *Pediatric research*, *61*(6), 653.

15. Björnholm, M., & Zierath, J. R. (2005). Insulin signal transduction in human skeletal muscle: identifying the defects in Type II diabetes.

16. Stump, C. S., Henriksen, E. J., Wei, Y., & Sowers, J. R. (2006). The metabolic syndrome: role of skeletal muscle metabolism. *Annals of medicine*, *38*(6), 389-402.

63

17. Kadowaki, T., Yamauchi, T., Kubota, N., Hara, K., Ueki, K., & Tobe, K. (2006). Adiponectin and adiponectin receptors in insulin resistance, diabetes, and the metabolic syndrome. *The Journal of clinical investigation*, *116*(7), 1784-1792.

18. Balsan, G. A., Vieira, J. L. D. C., Oliveira, A. M. D., & Portal, V. L. (2015). Relationship between adiponectin, obesity and insulin resistance. *Revista da Associação Médica Brasileira*, *61*(1), 72-80.

19. Pietrangelo, A. (2016). Iron and the liver. *Liver international*, *36*, 116-123.

20. Beard, J. L. (2001). Iron biology in immune function, muscle metabolism and neuronal functioning. *The Journal of nutrition*, *131*(2), 568S-580S.

21. Simcox, J. A., & McClain, D. A. (2013). Iron and diabetes risk. *Cell metabolism*, *17*(3), 329-341.

22. Rajpathak, S. N., Crandall, J. P., Wylie-Rosett, J., Kabat, G. C., Rohan, T. E., & Hu, F. B. (2009). The role of iron in type 2 diabetes in humans. *Biochimica et Biophysica Acta (BBA)-General Subjects*, *1790*(7), 671-681.

23. Puntarulo, S. (2005). Iron, oxidative stress and human health. *Molecular aspects of medicine*, *26*(4-5), 299-312.

24. Swaminathan, S., Fonseca, V. A., Alam, M. G., & Shah, S. V. (2007). The role of iron in diabetes and its complications. *Diabetes care*, *30*(7), 1926-1933.

25. Ford, E. S., & Cogswell, M. E. (1999). Diabetes and serum ferritin concentration among US adults. *Diabetes care*, *22*(12), 1978-1983.

26. Jehn, M., Clark, J. M., & Guallar, E. (2004). Serum ferritin and risk of the metabolic syndrome in US adults. *Diabetes care*, *27*(10), 2422-2428.

27. Piperno, A., Trombini, P., Gelosa, M., Mauri, V., Pecci, V., Vergani, A., ... & Mancia, G. (2002). Increased serum ferritin is common in men with essential hypertension. *Journal of hypertension*, *20*(8), 1513-1518.

28. Halle, M., König, D., Berg, A., Keul, J., & Baumstark, M. W. (1997). Relationship of serum ferritin concentrations with metabolic cardiovascular risk factors in men without evidence for coronary artery disease. *Atherosclerosis*, *128*(2), 235-240.

29. Tuomainen, T. P., Nyyssönen, K., Salonen, R., Tervahauta, A., Korpela, H., Lakka, T., ... & Salonen, J. T. (1997). Body iron stores are associated with serum insulin and blood glucose concentrations: population study in 1,013 eastern Finnish men. *Diabetes care*, *20*(3), 426-428.

30. Gillum RF: Association of serum ferritin and indices of body fat distribution and obesity in Mexican American men: the Third National Health and Nutrition Ex- amination Survey. *Int J Obes Relat Metab Disord* 25:639 – 645, 2001

31. Vari, I. S., Balkau, B., Kettaneh, A., André, P., Tichet, J., Fumeron, F., ... & Ducimetière, P. (2007). Ferritin and transferrin are associated with metabolic syndrome abnormalities and

their change over time in a general population: Data from an Epidemiological Study on the Insulin Resistance Syndrome (DESIR). *Diabetes Care*, *30*(7), 1795-1801.

32. Deugnier, Y., Bardou-Jacquet, É., & Lainé, F. (2017). Dysmetabolic iron overload syndrome (DIOS). *La Presse Médicale*, *46*(12), e306-e311.

33. Dongiovanni, P., Ruscica, M., Rametta, R., Recalcati, S., Steffani, L., Gatti, S., ... & Valenti, L. (2013). Dietary iron overload induces visceral adipose tissue insulin resistance. *The American journal of pathology*, *182*(6), 2254-2263.

34. Jorgensen, S. B., O'neill, H. M., Sylow, L., Honeyman, J., Hewitt, K. A., Palanivel, R., ... & van der Poel, C. (2013). Deletion of skeletal muscle SOCS3 prevents insulin resistance in obesity. *Diabetes*, *62*(1), 56-64.

35. Kehrer, J. P. (2000). The Haber–Weiss reaction and mechanisms of toxicity. *Toxicology*, *149*(1), 43-50.

36. Kadowaki, T., & Yamauchi, T. (2005). Adiponectin and adiponectin receptors. *Endocrine reviews*, *26*(3), 439-451.

37. Kadowaki, T., Yamauchi, T., Kubota, N., Hara, K., Ueki, K., & Tobe, K. (2006). Adiponectin and adiponectin receptors in insulin resistance, diabetes, and the metabolic syndrome. *The Journal of clinical investigation*, *116*(7), 1784-1792.

38. Caselli, C. (2014). Role of adiponectin system in insulin resistance. *Molecular genetics and metabolism*, *113*(3), 155-160.

39. Balsan, G. A., Vieira, J. L. D. C., Oliveira, A. M. D., & Portal, V. L. (2015). Relationship between adiponectin, obesity and insulin resistance. *Revista da Associação Médica Brasileira*, *61*(1), 72-80.

40. Turer, A. T., & Scherer, P. E. (2012). Adiponectin: mechanistic insights and clinical implications. *Diabetologia*, *55*(9), 2319-2326.

41. Achari, A., & Jain, S. (2017). Adiponectin, a therapeutic target for obesity, diabetes, and endothelial dysfunction. *International journal of molecular sciences*, *18*(6), 1321.

42. Buechler, C., Wanninger, J., & Neumeier, M. (2010). Adiponectin receptor binding proteins– recent advances in elucidating adiponectin signalling pathways. *FEBS letters*, *584*(20), 4280-4286.

43. Deepa, S. S., & Dong, L. Q. (2009). APPL1: role in adiponectin signaling and beyond. *American Journal of Physiology-Endocrinology and Metabolism*, *296*(1), E22-E36.

44. Mao, X., Kikani, C. K., Riojas, R. A., Langlais, P., Wang, L., Ramos, F. J., ... & Liu, F. (2006). APPL1 binds to adiponectin receptors and mediates adiponectin signalling and function. *Nature cell biology*, *8*(5), 516.

45. Yamauchi, T., Kamon, J., Minokoshi, Y. A., Ito, Y., Waki, H., Uchida, S., ... & Eto, K. (2002). Adiponectin stimulates glucose utilization and fatty-acid oxidation by activating AMP-activated protein kinase. *Nature medicine*, *8*(11), 1288.

46. Zhou, L., Deepa, S. S., Etzler, J. C., Ryu, J., Mao, X., Fang, Q., ... & Liu, F. (2009). Adiponectin activates AMP-activated protein kinase in muscle cells via APPL1/LKB1-dependent and phospholipase C/Ca2+/Ca2+/calmodulin-dependent protein kinase kinase-dependent pathways. *Journal of Biological Chemistry, 284*(33), 22426-22435.

47. Wang, Y., Ma, X. L., & Lau, W. B. (2017). Cardiovascular adiponectin resistance: the critical role of adiponectin receptor modification. *Trends in Endocrinology & Metabolism, 28*(7), 519-530.

48. Yoon, M. J., Lee, G. Y., Chung, J. J., Ahn, Y. H., Hong, S. H., & Kim, J. B. (2006). Adiponectin increases fatty acid oxidation in skeletal muscle cells by sequential activation of AMP-activated protein kinase, p38 mitogen-activated protein kinase, and peroxisome proliferator–activated receptor α. *Diabetes*, *55*(9), 2562-2570.

49. Yamauchi, T., Iwabu, M., Okada-Iwabu, M., & Kadowaki, T. (2014). Adiponectin receptors: a review of their structure, function and how they work. *Best practice & research Clinical endocrinology & metabolism*, *28*(1), 15-23.

50. Cuadrado, A., & Nebreda, A. R. (2010). Mechanisms and functions of p38 MAPK signalling. *Biochemical Journal, 429*(3), 403-417.

51. Zarubin, T., & Jiahuai, H. A. N. (2005). Activation and signaling of the p38 MAP kinase pathway. *Cell research*, *15*(1), 11.

52. Xin, X., Zhou, L., Reyes, C. M., Liu, F., & Dong, L. Q. (2010). APPL1 mediates adiponectin-stimulated p38 MAPK activation by scaffolding the TAK1-MKK3-p38 MAPK pathway. *American Journal of Physiology-Endocrinology and Metabolism*, *300*(1), E103-E110.

53. Xi, X., Han, J., & Zhang, J. Z. (2001). Stimulation of glucose transport by AMP-activated protein kinase via activation of p38 mitogen-activated protein kinase. *Journal of Biological Chemistry*, *276*(44), 41029-41034.

54. Asada, S., Daitoku, H., Matsuzaki, H., Saito, T., Sudo, T., Mukai, H., ... & Fukamizu, A. (2007). Mitogen-activated protein kinases, Erk and p38, phosphorylate and regulate Foxo1. *Cellular signalling*, *19*(3), 519-527.

55. Zhao, Y., Wang, Y., & Zhu, W. G. (2011). Applications of post-translational modifications of FoxO family proteins in biological functions. *Journal of molecular cell biology*, *3*(5), 276-282.

56. Lundell, L. S., Massart, J., Altıntaş, A., Krook, A., & Zierath, J. R. (2019). Regulation of glucose uptake and inflammation markers by FOXO1 and FOXO3 in skeletal muscle. *Molecular metabolism*, *20*, 79-88.

57. Ponugoti, B., Dong, G., & Graves, D. T. (2012). Role of forkhead transcription factors in diabetes-induced oxidative stress. *Experimental diabetes research*, *2012*.

58. Matsuzaki, H., Daitoku, H., Hatta, M., Tanaka, K., & Fukamizu, A. (2003). Insulin-induced phosphorylation of FKHR (Foxo1) targets to proteasomal degradation. *Proceedings of the National Academy of Sciences*, *100*(20), 11285-11290.

59. Tsuchida, A., Yamauchi, T., Ito, Y., Hada, Y., Maki, T., Takekawa, S., ... & Kubota, N. (2004). Insulin/Foxo1 pathway regulates expression levels of adiponectin receptors and adiponectin sensitivity. *Journal of Biological Chemistry*, *279*(29), 30817-30822.

60. Sattar, A. A., & Sattar, R. (2012). Insulin-regulated expression of adiponectin receptors in muscle and fat cells. *Cell biology international*, *36*(12), 1293-1297.

61. Yamauchi, T., Kamon, J., Waki, H., Terauchi, Y., Kubota, N., Hara, K., . . . Tsuboyama-Kasaoka, N. (2001). The fat-derived hormone adiponectin reverses insulin resistance associated with both lipoatrophy and obesity. *Nature medicine, 7*(8), 941

62. Barthel, A., Schmoll, D., & Unterman, T. G. (2005). FoxO proteins in insulin action and metabolism. *Trends in Endocrinology & Metabolism, 16*(4), 183-189

63. Gabrielsen, J. S., Gao, Y., Simcox, J. A., Huang, J., Thorup, D., Jones, D., ... & Hopkins, P. N. (2012). Adipocyte iron regulates adiponectin and insulin sensitivity. *The Journal of clinical investigation, 122*(10), 3529Barthel, A., Schmoll, D., & Unterman, T. G. (2005).

FoxO proteins in insulin action and metabolism. *Trends in Endocrinology & Metabolism*, *16*(4), 183-189.

64. Mullen, K. L., Pritchard, J., Ritchie, I., Snook, L. A., Chabowski, A., Bonen, A., ... & Dyck, D. J. (2009). Adiponectin resistance precedes the accumulation of skeletal muscle lipids and insulin resistance in high-fat-fed rats. *American Journal of Physiology-Regulatory, Integrative and Comparative Physiology*, *296*(2), R243-R251.
65. Sente, T., Van Berendoncks, A. M., Hoymans, V. Y., & Vrints, C. J. (2016). Adiponectin resistance in skeletal muscle: pathophysiological implications in chronic heart failure. *Journal of cachexia, sarcopenia and muscle*, *7*(3), 261-274.
66. Bruce, C. R., Mertz, V. A., Heigenhauser, G. J., & Dyck, D. J. (2005). The stimulatory effect of globular adiponectin on insulin-stimulated glucose uptake and fatty acid oxidation is impaired in skeletal muscle from obese subjects. *Diabetes*, *54*(11), 3154-3160.
67. Jiang, R., Manson, J. E., Meigs, J. B., Ma, J., Rifai, N., & Hu, F. B. (2004). Body iron stores in relation to risk of type 2 diabetes in apparently healthy women. *Jama, 291*(6), 711-717
68. Fernández-Real, J. M., Lopez-Bermejo, A., & Ricart, W. (2005). Iron stores, blood donation, and insulin sensitivity and secretion. *Clinical chemistry, 51*(7), 1201-1205
69. Ascherio, A., Rimm, E. B., Giovannucci, E., Willett, W. C., & Stampfer, M. J. (2001). Blood donations and risk of coronary heart disease in men. *Circulation, 103*(1), 52-57.
70. Zheng, H., Patel, M., Cable, R., Young, L., & Katz, S. D. (2007). Insulin sensitivity, vascular function, and iron stores in voluntary blood donors. *Diabetes care, 30*(10), 2685-2689.
71. Facchini, F. S., & Saylor, K. L. (2002). Effect of iron depletion on cardiovascular risk factors. *Annals of the New York Academy of Sciences, 967*(1), 342-351.
72. Huang, J., Jones, D., Luo, B., Sanderson, M., Soto, J., Abel, E. D., . . . McClain, D. A. (2011). Iron overload and diabetes risk: a shift from glucose to fatty acid oxidation and increased hepatic glucose production in a mouse model of hereditary hemochromatosis. *Diabetes, 60*(1), 80-87
73. Halasi, M., Wang, M., Chavan, T. S., Gaponenko, V., Hay, N., & Gartel, A. L. (2013). ROS inhibitor N-acetyl-L-cysteine antagonizes the activity of proteasome inhibitors. *Biochemical Journal, 454*(2), 201-208
74. Kusminski, C. M., Holland, W. L., Sun, K., Park, J., Spurgin, S. B., Lin, Y., . . . Li, C. (2012). MitoNEET, a key regulator of mitochondrial function and lipid homeostasis. *Nature medicine, 18*(10), 1539.
75. Petersen, K. F., Dufour, S., Savage, D. B., Bilz, S., Solomon, G., Yonemitsu, S., . . . Kahn, B. B. (2007). The role of skeletal muscle insulin resistance in the pathogenesis of the metabolic syndrome. *Proceedings of the National Academy of Sciences, 104*(31), 12587-12594
76. Charlton, H. K., Webster, J., Kruger, S., Simpson, F., Richards, A. A., & Whitehead, J. P. (2010). ERp46 binds to AdipoR1, but not AdipoR2, and modulates adiponectin signalling. *Biochemical and biophysical research communications, 392*(2), 234-23
77. Henderson, R. J., Patton, S. M., & Connor, J. R. (2005). Development of a fluorescent reporter to assess iron regulatory protein activity in living cells. *Biochimica et Biophysica Acta (BBA)-Molecular Cell Research*, *1743*(1-2), 162-168.
78. Park, H. J., Kang, Y. M., Kim, C. H., & Jung, M. H. (2010). ATF3 negatively regulates adiponectin receptor 1 expression. *Biochemical and biophysical research communications*, *400*(1), 72-77.
79. Saklayen, M. G. (2018). The global epidemic of the metabolic syndrome. *Current hypertension reports, 20*(2), 12.

80. Palmer, M. K., & Toth, P. P. (2019). Trends in Lipids, Obesity, Metabolic Syndrome, and Diabetes Mellitus in the United States: An NHANES Analysis (2003-2004 to 2013-2014). *Obesity*, *27*(2), 309-314.

81. Straub, L. G., & Scherer, P. E. (2019). Metabolic Messengers: adiponectin. *Nature Metabolism, 1*(3), 334

82. Ryu, J., Galan, A. K., Xin, X., Dong, F., Abdul-Ghani, M. A., Zhou, L., ... & Austad, S. N. (2014). APPL1 potentiates insulin sensitivity by facilitating the binding of IRS1/2 to the insulin receptor. *Cell reports*, *7*(4), 1227-1238.

83. Grundy, S. M. (2018). *Metabolic syndrome*: Springer

84. Sung, H. K., Song, E., Jahng, J. W. S., Pantopoulos, K., & Sweeney, G. (2019). Iron induces insulin resistance in cardiomyocytes via regulation of oxidative stress. *Scientific reports, 9*(1), 4668

85. Suárez-Ortegón, M., Blanco, E., McLachlan, S., Fernandez-Real, J., Burrows, R., Wild, S., . . . Gahagan, S. (2019). Ferritin levels throughout childhood and metabolic syndrome in adolescent stage. *Nutrition, Metabolism and Cardiovascular Diseases, 29*(3), 268-278

86. Gutteridge, J. M., & Halliwell, B. (2018). Mini-Review: Oxidative stress, redox stress or redox success? *Biochemical and biophysical research communications, 502*(2), 183-186

87. Aregbesola, A., de Mello, V. D., Lindström, J., Voutilainen, S., Virtanen, J. K., Keinänen-Kiukaanniemi, S., . . . Uusitupa, M. (2018). Serum adiponectin/Ferritin ratio in relation to the risk of type 2 diabetes and insulin sensitivity. *Diabetes research and clinical practice, 141*, 264-274.

88. Unterman, T. G. (2018). Regulation of Hepatic Glucose Metabolism by FoxO Proteins, an Integrated Approach. In *Current topics in developmental biology* (Vol. 127, pp. 119-147): Elsevier

89. Rajan, M. R., Nyman, E., Brännmark, C., Olofsson, C. S., & Strålfors, P. (2018). Inhibition of FOXO1 transcription factor in primary human adipocytes mimics the insulin-resistant state of type 2 diabetes. *Biochemical Journal, 475*(10), 1807-1820.

90. Shikatani, E. A., Trifonova, A., Mandel, E. R., Liu, S. T., Roudier, E., Krylova, A., . . . Haas, T. L. (2012). Inhibition of proliferation, migration and proteolysis contribute to corticosterone-mediated inhibition of angiogenesis. *PloS one, 7*(10), e46625

91. Forouhi, N., Harding, A., Allison, M., Sandhu, M., Welch, A., Luben, R., . . . Wareham, N. (2007). Elevated serum ferritin levels predict new-onset type 2 diabetes: results from the EPIC-Norfolk prospective study. *Diabetologia, 50*(5), 949-956

92. Jehn, M. L., Guallar, E., Clark, J. M., Couper, D., Duncan, B. B., Ballantyne, C. M., . . . Pankow, J. S. (2007). A prospective study of plasma ferritin level and incident diabetes: the Atherosclerosis Risk in Communities (ARIC) Study. *American journal of epidemiology, 165*(9), 1047-1054.

93. Salonen, J. T., Tuomainen, T.-P., Nyyssönen, K., Lakka, H.-M., & Punnonen, K. (1998). Relation between iron stores and non-insulin dependent diabetes in men: case-control study. *Bmj, 317*(7160), 727-730

94. Fumeron, F., Péan, F., Driss, F., Balkau, B., Tichet, J., Marre, M., & Grandchamp, B. (2006). Ferritin and transferrin are both predictive of the onset of hyperglycemia in men and women over 3 years: the data from an epidemiological study on the Insulin Resistance Syndrome (DESIR) study. *Diabetes care, 29*(9), 2090-2094

95. Kido, K., Ato, S., Yokokawa, T., Sato, K., & Fujita, S. (2018). Resistance training recovers attenuated APPL1 expression and improves insulin-induced Akt signal activation in skeletal muscle of type 2 diabetic rats. *American Journal of Physiology-Endocrinology and Metabolism, 314*(6), E564-E571

96. Lowell, B. B., & Shulman, G. I. (2005). Mitochondrial dysfunction and type 2 diabetes. *Science*, *307*(5708), 384-387.

97. Hu, J., Kholmukhamedov, A., Lindsey, C. C., Beeson, C. C., Jaeschke, H., & Lemasters, J. J. (2016). Translocation of iron from lysosomes to mitochondria during acetaminophen-induced hepatocellular injury: protection by starch-desferal and minocycline. *Free Radical Biology and Medicine*, *97*, 418-426.

98. Li, N., Ragheb, K., Lawler, G., Sturgis, J., Rajwa, B., Melendez, J. A., & Robinson, J. P. (2003). Mitochondrial complex I inhibitor rotenone induces apoptosis through enhancing mitochondrial reactive oxygen species production. *Journal of Biological Chemistry*, *278*(10), 8516-8525.

99. Dumay, A., Rincheval, V., Trotot, P., Mignotte, B., & Vayssière, J. L. (2006). The superoxide dismutase inhibitor diethyldithiocarbamate has antagonistic effects on apoptosis by triggering both cytochrome c release and caspase inhibition. *Free Radical Biology and Medicine*, *40*(8), 1377-1390.

100. Lane, D. J. R., Merlot, A. M., Huang, M. H., Bae, D. H., Jansson, P. J., Sahni, S., ... & Richardson, D. R. (2015). Cellular iron uptake, trafficking and metabolism: key molecules and mechanisms and their roles in disease. *Biochimica et Biophysica Acta (BBA)-Molecular Cell Research*, *1853*(5), 1130-1144.

101. Ji, C., & Kosman, D. J. (2015). Molecular mechanisms of non-transferrin-bound and transferring-bound iron uptake in primary hippocampal neurons. *Journal of neurochemistry*, *133*(5), 668-683.